CSIAM Trans. Appl. Math.
doi: 10.4208/csiam-am.SO-2021-0022

Vol. **4**, No. 2, pp. 345-380
June 2023

Convergence Analysis on a Structure-Preserving Numerical Scheme for the Poisson-Nernst-Planck-Cahn-Hilliard System

Yiran Qian[1], Cheng Wang[2] and Shenggao Zhou[3,*]

[1] *School of Mathematical Sciences, Suzhou University of Science and Technology, Suzhou 215009, P.R. China.*
[2] *Department of Mathematics, University of Massachusetts, North Dartmouth, MA 02747, USA.*
[3] *School of Mathematical Sciences, MOE-LSC, and CMAI-Shanghai, Shanghai Jiao Tong University, Shanghai, P.R. China.*

Received 1 April 2022; Accepted 29 November 2022

Abstract. In this paper, we provide an optimal rate convergence analysis and error estimate for a structure-preserving numerical scheme for the Poisson-Nernst-Planck-Cahn-Hilliard (PNPCH) system. The numerical scheme is based on the Energetic Variational Approach of the physical model, which is reformulated as a non-constant mobility gradient flow of a free-energy functional that consists of singular logarithmic energy potentials arising from the PNP theory and the Cahn-Hilliard surface diffusion process. The mobility function is explicitly updated, while the logarithmic and the surface diffusion terms are computed implicitly. The primary challenge in the development of theoretical analysis on optimal error estimate has been associated with the nonlinear parabolic coefficients. To overcome this subtle difficulty, an asymptotic expansion of the numerical solution is performed, so that a higher order consistency order can be obtained. The rough error estimate leads to a bound in maximum norm for concentrations, which plays an essential role in the nonlinear analysis. Finally, the refined error estimate is carried out, and the desired convergence estimate is accomplished. Numerical results are presented to demonstrate the convergence order and performance of the numerical scheme in preserving physical properties and capturing ionic steric effects in concentrated electrolytes.

AMS subject classifications: 35K35, 35K55, 65M06, 65M12

Key words: Poisson-Nernst-Planck-Cahn-Hilliard system, positivity preserving, optimal rate convergence analysis, higher order asymptotic expansion, rough error estimate, refined error estimate.

---

*Corresponding author. *Email addresses:* `yrqian@usts.edu.cn` (Y. Qian), `cwang1@umassd.edu` (C. Wang), `sgzhou@sjtu.edu.cn` (S. Zhou)

1 Introduction

The well-known Poisson-Nernst-Planck (PNP) theory has been widely applied to describe the ion transport in many biological processes and technological applications, such as ion channels, semiconductors, and electric double layer capacitors [2, 4, 40, 60]. Although it has achieved great success in many applications, the PNP theory has many limitations due to its mean-field nature. In the mean-field approximation, ions are treated as point charges that only interact with the background electric potential arising from the charges in the system. As such, ionic steric effect and ion-ion correlation have been ignored. However, such ignored effects could be crucial to description of ion transport in some scenarios, e.g., charge dynamics in concentrated electrolytes and ions permeation through ion channels.

To overcome the limitations, various modified PNP theories with steric effects have been proposed recently. Based on a lattice gas model, ionic steric effect has been taken into account through the incorporation of entropy of solvent molecules to the electrostatic free energy [6, 31–34, 39, 44, 61]. Another approach is to consider steric effects via including the Lennard-Jones potential for hard-sphere repulsions [18,30,36]. To avoid computationally inefficient integro-differential equations, local approximations of nonlocal terms up to the leading order have been proposed to get reduced local models [28, 30, 36]. To get more accurate models, regularization terms of concentration gradient energies can be further included to describe the steric interactions [20–23]. The proposal of such concentration gradient terms follows the same spirit as the Ginzburg-Landau theory for the description of phase separation in mixtures.

Considering an H^{-1} gradient flow of the electrostatic free energy with the additional concentration gradient energies, one can obtain the following Poisson-Nernst-Planck-Cahn-Hilliard (PNPCH) system:

$$\begin{cases} \dfrac{\partial c^l}{\partial t} = D^l \nabla \cdot \left[c^l \nabla \left(z^l \phi + \ln c^l + \displaystyle\sum_{n=1}^{M} g^{ln} c^n - \sigma^l \Delta c^l \right) \right], & l = 1,2,\ldots,M, \\ -\nabla \cdot (\kappa \nabla \phi) = \displaystyle\sum_{l=1}^{M} z^l c^l + \rho^f, \end{cases}$$

where ϕ is the electrostatic potential, c^l is the ion concentration for the l-th species, z^l is the valence, M is the total number of the ionic species, ρ^f is the fixed charge density, κ and D^l are coefficients arising from nondimensionalization, $G = (g^{ln})$ is the coefficient matrix for steric interactions, and σ^l is a gradient energy coefficient. Since its proposal in the work [20], the PNPCH system has been applied to study the ion transport in ion channels [22] and charge dynamics in room temperature ionic liquids [21, 23].

In this work, we consider structure-preserving numerical methods and their error estimates for the PNPCH system. For simplicity of presentation, we assume a homogeneous source term $\rho^f \equiv 0$, and $M = 2$, which corresponds to only two species of ions, denoted as n and p. The analysis of this work could be easily extended to the case of multi concentrations and non-homogeneous source terms. In addition, we set $D_n=1$, $\kappa=1$, $z^n=-1$, and $z^p=1$, after a careful scaling process. In turn, the two-species PNPCH system could be rewritten as

$$\partial_t n=\nabla\cdot\big(n\nabla(-\phi+\ln n+g_{11}n+g_{12}p-\sigma^n\Delta n)\big), \tag{1.1}$$

$$\partial_t p=\nabla\cdot\big(Dp\nabla(\phi+\ln p+g_{21}n+g_{22}p-\sigma^p\Delta p)\big), \tag{1.2}$$

$$-\Delta\phi=p-n, \tag{1.3}$$

in which $G=(g_{i,j})$ is a 2×2 symmetric matrix. Periodic boundary conditions are imposed for the PNPCH system (1.1)-(1.3). After nondimensionalization, the free energy of the charged system is formulated as

$$E(n,p)=\int_\Omega\left\{n\ln n+p\ln p+(n,p)G(n,p)^T+\frac{1}{2}\sigma^n|\nabla n|^2+\frac{1}{2}\sigma^p|\nabla p|^2\right\}d\mathbf{x}+\frac{1}{2}\|n-p\|^2_{H^{-1}}, \tag{1.4}$$

and the PDE system (1.1)-(1.3) turns out to be the following conserved gradient flow:

$$\partial_t n=\nabla\cdot(n\nabla\mu_n),\quad \partial_t p=D\nabla\cdot\big(p\nabla\mu_p\big). \tag{1.5}$$

In more details, μ_n and μ_p are the dimensionless chemical potentials calculated as

$$\mu_n:=\delta_n E=\ln n+1+(-\Delta)^{-1}(n-p)+g_{11}n+g_{12}p-\sigma^n\Delta n, \tag{1.6}$$

$$\mu_p:=\delta_p E=\ln p+1+(-\Delta)^{-1}(p-n)+g_{21}n+g_{22}p-\sigma^p\Delta p, \tag{1.7}$$

and ϕ is the solution to $-\Delta\phi=p-n$, with periodic boundary conditions. In fact, the energy dissipation law could be derived as

$$d_tE=-\int_\Omega\left\{n|\nabla\mu_n|^2+Dp|\nabla\mu_p|^2\right\}d\mathbf{x}\le 0.$$

Recent years have seen great progress on the development of structure-preserving numerical methods for the classical PNP-type equations [9, 10, 19, 27, 29, 37, 38, 48, 49]. For instance, a second-order accurate and energy dissipative finite difference method based on a Slotboom transformation was proposed for the PNP equations in one dimension [38]. A positivity-preserving finite element scheme that uses the logarithm of concentrations as unknowns was developed for the PNP-type equations [41]. Another category of structure-preserving numerical methods was developed based on a gradient-flow structure of the PNP equations. For instance, implicit numerical schemes that unconditionally ensure positivity, unique solvability, and energy dissipation were proposed for a class of the Keller-Segel equations [47] and PNP equations [48]. Unconditional structure-preserving finite difference schemes, along with convergence analysis, were developed for the classical PNP equations [37].

The existing works of numerical methods for the PNPCH system (1.1)-(1.3) have been very limited. It is worthy of mentioning a recent article [43], in which a finite difference scheme is proposed. The mobility function is explicitly updated in the numerical scheme, so that the unique solvability analysis has been facilitated. In the numerical approximation of chemical potentials, both the logarithmic and the surface diffusion terms are computed implicitly, since these two terms turn out to be the gradient of convex nature energy parts. For the steric interaction terms, a convex-concave decomposition is available, and the convex splitting numerical approach is applied. The positivity preserving property has been established at a theoretical level for the resulting numerical algorithm, i.e., $n>0$ and $p>0$, is satisfied at a theoretical level, so that the numerical solution is well-defined in the energetic variational formulation. Moreover, an unconditional energy stability analysis has also been proved for the numerical scheme. Similar ideas have been applied to the other gradient model with singular energy potential, such as the Cahn-Hilliard equation with Flory-Huggins energy potential [7, 12–14], the Poisson-Nernst-Planck system [37, 43], liquid film droplet model [59], etc.

On the other hand, an optimal rate convergence analysis has been an open problem for the PNPCH system (1.1)-(1.3), and we will provide such an analysis for the finite difference scheme proposed in [43]. The primary challenge is associated with the non-constant mobility in the variational structure, as well as the singular and nonlinear nature of the logarithmic terms in the chemical potential expansions. In comparison, many existing works of convergence estimate for the PNP system [8, 42, 50] has been based on a perfect Laplacian operator; as a result, the variational structure is broken and an energy stability analysis is not available for these numerical approaches. To overcome the difficulty in terms of non-constant mobility and singular logarithmic chemical potential terms, we have to make use of several non-standard techniques to control the nonlinear parabolic coefficients. A careful calculation reveals that, a uniform distance between the numerical solution and the singular limit value is needed to pass through the error estimate if a nonlinear mobility function is involved with a singular logarithmic energy potential. In fact, such a phase separation property is available for the exact PDE solution, and we are able to obtain a similar property with an application of a-priori estimates. Meanwhile, the leading order truncation error is not sufficient to establish the required separation property, due to the first order temporal accuracy of the numerical scheme. To avoid such an insufficiency, we apply the technique of higher order asymptotic expansion for the numerical solution, based on a careful linearization approach. In turn, the constructed approximate solution satisfy the numerical scheme with a higher order consistency order, up to the second order temporal accuracy. Subsequently, this higher order consistency analysis, combined with the convex nature of the nonlinear logarithmic terms, enables one to derive a rough error estimate. As a consequence of the rough error estimate, the ℓ^∞ bound for both ion concentration variables could be derived, as well as their discrete $W^{1,4}$ bounds. These bounds play a crucial role in the refined error estimate, in which the desired convergence result could be established afterward.

The rest of the article is organized as follows. In Section 2, we review the numerical scheme, and state the main theoretical results. The high order consistency analysis is presented in Section 3, the rough error estimate is provided in Section 4, and the refined error estimate is established in Section 5. Some numerical results are provided in Section 6. Finally, the concluding remarks are given in Section 7.

2 Numerical scheme and main theoretical results

2.1 The finite difference spatial discretization

The standard centered finite difference spatial approximation is applied. We present the numerical approximation on the computational domain $\Omega=(0,1)^3$ with a periodic boundary condition, and $\Delta x=\Delta y=\Delta z=h=1/N$ with $N\in\mathbb{N}$ to be the spatial mesh resolution throughout this work. In particular, $f_{i,j,k}$ stands for the numerical value of f at the cell centered mesh points $((i+1/2)h,(j+1/2)h,(k+1/2)h)$, and we denote $\mathcal{C}_{\rm per}$ as

$$\mathcal{C}_{\rm per}:=\left\{(f_{i,j,k})\,|\,f_{i,j,k}=f_{i+\alpha N,j+\beta N,k+\gamma N},\ \forall i,j,k,\alpha,\beta,\gamma\in\mathbb{Z}\right\}$$

with the discrete periodic boundary condition imposed. In turn, the discrete average and difference operators are evaluated at $(i+1/2,j,k)$, $(i,j+1/2,k)$ and $(i,j,k+1/2)$, respectively

$$\begin{aligned}
&A_x f_{i+\frac12,j,k}:=\frac12\left(f_{i+1,j,k}+f_{i,j,k}\right), \quad D_x f_{i+\frac12,j,k}:=\frac1h\left(f_{i+1,j,k}-f_{i,j,k}\right),\\
&A_y f_{i,j+\frac12,k}:=\frac12\left(f_{i,j+1,k}+f_{i,j,k}\right), \quad D_y f_{i,j+\frac12,k}:=\frac1h\left(f_{i,j+1,k}-f_{i,j,k}\right),\\
&A_z f_{i,j,k+\frac12}:=\frac12\left(f_{i,j,k+1}+f_{i,j,k}\right), \quad D_z f_{i,j,k+\frac12}:=\frac1h\left(f_{i,j,k+1}-f_{i,j,k}\right).
\end{aligned}$$

The corresponding operators at the staggered mesh points are defined as follows:

$$\begin{aligned}
&a_x f^x_{i,j,k}:=\frac12\left(f^x_{i+\frac12,j,k}+f^x_{i-\frac12,j,k}\right), \quad d_x f^x_{i,j,k}:=\frac1h\left(f^x_{i+\frac12,j,k}-f^x_{i-\frac12,j,k}\right),\\
&a_y f^y_{i,j,k}:=\frac12\left(f^y_{i,j+\frac12,k}+f^y_{i,j-\frac12,k}\right), \quad d_y f^y_{i,j,k}:=\frac1h\left(f^y_{i,j+\frac12,k}-f^y_{i,j-\frac12,k}\right),\\
&a_z f^z_{i,j,k}:=\frac12\left(f^z_{i,j,k+\frac12}+f^z_{i,j,k-\frac12}\right), \quad d_z f^z_{i,j,k}:=\frac1h\left(f^z_{i,j,k+\frac12}-f^z_{i,j,k-\frac12}\right).
\end{aligned}$$

In turn, for a scalar cell-centered function g and a vector function $\vec{f}=(f^x,f^y,f^z)^T$, with f^x, f^y and f^z evaluated at $(i+1/2,j,k)$, $(i,j+1/2,k)$, $(i,j,k+1/2)$, respectively, the discrete divergence is defined as

$$\nabla_h\cdot\left(g\vec{f}\right)_{i,j,k}=d_x\left(A_xg\cdot f^x\right)_{i,j,k}+d_y\left(A_yg\cdot f^y\right)_{i,j,k}+d_z\left(A_zg\cdot f^z\right)_{i,j,k}. \tag{2.1}$$

In particular, if $\vec{f}=\nabla_h\phi=(D_x\phi,D_y\phi,D_z\phi)^T$ for certain scalar grid function ϕ, the corresponding divergence becomes

$$\nabla_h\cdot\left(g\nabla_h\phi\right)_{i,j,k}=d_x\left(A_xg\cdot D_x\phi\right)_{i,j,k}+d_y\left(A_yg\cdot D_y\phi\right)_{i,j,k}+d_z\left(A_zg\cdot D_z\phi\right)_{i,j,k}, \tag{2.2}$$

$$(\Delta_h\phi)_{i,j,k}=\nabla_h\cdot\left(\nabla_h\phi\right)_{i,j,k}=d_x\left(D_x\phi\right)_{i,j,k}+d_y\left(D_y\phi\right)_{i,j,k}+d_z\left(D_z\phi\right)_{i,j,k}. \tag{2.3}$$

For two cell-centered grid functions f and g, its discrete L^2 inner product and the associated ℓ^2 norm are defined as

$$\langle f,g\rangle_\Omega := h^3 \sum_{i,j,k=1}^{N} f_{i,j,k} g_{i,j,k}, \quad \|f\|_2 := \left(\langle f,f\rangle_\Omega\right)^{\frac{1}{2}}.$$

In turn, the mean zero space is introduced as

$$\mathring{\mathcal{C}}_{\rm per} := \left\{ f\in\mathcal{C}_{\rm per} \,\middle|\, 0=\overline{f} := \frac{h^3}{|\Omega|}\sum_{i,j,k=1}^{m} f_{i,j,k} \right\}.$$

Similarly, for two vector grid functions $\vec{f}=(f^x,f^y,f^z)^T$, $\vec{g}=(g^x,g^y,g^z)^T$, with $f^x(g^x)$, $f^y(g^y)$, $f^z(g^z)$ evaluated at $(i+1/2,j,k)$, $(i,j+1/2,k)$, $(i,j,k+1/2)$, respectively, the corresponding discrete inner product becomes

$$\begin{aligned}
&[\vec{f},\vec{g}] := [f^x,g^x]_{\rm x} + [g^y,g^y]_{\rm y} + [f^z,g^z]_{\rm z},\\
&[f^x,g^x]_{\rm x} := \langle a_x(f^x g^x),1\rangle, \quad [f^y,g^y]_{\rm y} := \langle a_y(f^y g^y),1\rangle, \quad [f^z,g^z]_{\rm z} := \langle a_z(f^z g^z),1\rangle.
\end{aligned}$$

In addition to the discrete $\|\cdot\|_2$ norm, the discrete maximum norm is defined as

$$\|f\|_\infty := \max_{1\le i,j,k\le N} |f_{i,j,k}|.$$

Moreover, the discrete H_h^1 and H_h^2 norms are introduced as

$$\begin{aligned}
&\|\nabla_h f\|_2^2 := [\nabla_h f,\nabla_h f] = [D_x f,D_x f]_{\rm x} + \left[D_y f,D_y f\right]_{\rm y} + [D_z f,D_z f]_{\rm z},\\
&\|f\|_{H_h^1}^2 := \|f\|_2^2 + \|\nabla_h f\|_2^2, \quad \|f\|_{H_h^2}^2 := \|f\|_{H_h^1}^2 + \|\Delta_h f\|_2^2.
\end{aligned}$$

The summation by parts formulas are recalled in the following lemma; the detailed proof could be found in [26, 55, 57, 58].

Lemma 2.1 ([26, 55, 57, 58])**.** *For any $\psi,\phi,g\in\mathcal{C}_{\rm per}$, and any $\vec{f}=(f^x,f^y,f_z)^T$, with f^x, f^y, f^z evaluated at $(i+1/2,j,k)$, $(i,j+1/2,k)$, $(i,j,k+1/2)$, respectively, the following summation by parts formulas are valid:*

$$\left\langle \psi\nabla_h\cdot\vec{f}\right\rangle = -\left[\nabla_h\psi,\vec{f}\right], \quad \left\langle \psi,\nabla_h\cdot(g\nabla_h\phi)\right\rangle = -\left[\nabla_h\psi,\mathcal{A}_h g\nabla_h\phi\right], \tag{2.4}$$

in which $\mathcal{A}_h$ corresponds to the average operator given by A_x, A_y and A_z.

A discrete Sobolev embedding from H_h^2 into ℓ^∞ has been proved in [11]. This inequality will be useful in the later convergence analysis.

Lemma 2.2 ([11])**.** *For any 3-D periodic grid function f (over cell centered mesh points), we have*

$$\|f\|_\infty \le C\left(\|f\|_2 + \|\Delta_h f\|_2\right). \tag{2.5}$$

In addition, we denote C_1 as the constant associated with the discrete Poincaré inequality

$$\|\nabla_h f\|_2 \geq C_1 \|f\|_2 \quad \text{for any} \quad f \quad \text{with} \quad \overline{f}=0. \tag{2.6}$$

Remark 2.1. For ease of presentation, we consider periodic boundary conditions in the numerical analysis. The numerical scheme and corresponding analysis can be extended to homogenous Neumann boundary conditions. For non-homogeneous ones, the mass conservation and energy dissipation properties should be accordingly modified and the auxiliary functions can be introduced to deal with the non-homogeneous boundary data. For more complicated boundary conditions, the convergence analysis is more mathematically involved and will be considered in our future work.

2.2 Review of numerical scheme and properties

The following finite difference scheme has been proposed in a recent work [43]: given $n^m, p^m \in \mathcal{C}_{\rm per}$, find $n^{m+1}, p^{m+1} \in \mathcal{C}_{\rm per}$ such that

$$\begin{aligned}
&\frac{n^{m+1}-n^m}{\Delta t} = \nabla_h \cdot \left(\check{\mathcal{M}}_n^m \nabla_h \mu_n^{m+1} \right), && (2.7)\\
&\frac{p^{m+1}-p^m}{\Delta t} = \nabla_h \cdot \left(\check{\mathcal{M}}_p^m \nabla_h \mu_p^{m+1} \right), && (2.8)\\
&\mu_n^{m+1} = \ln n^{m+1} + (-\Delta_h)^{-1}\left(n^{m+1}-p^{m+1}\right) + g_{11}^c n^{m+1} + g_{12}^c p^{m+1} \\
&\qquad - g_{11}^e n^m - g_{12}^e p^m - \sigma^n \Delta_h n^{m+1}, && (2.9)\\
&\mu_p^{m+1} = \ln p^{m+1} + (-\Delta_h)^{-1}\left(p^{m+1}-n^{m+1}\right) + g_{21}^c n^{m+1} + g_{22}^c p^{m+1} \\
&\qquad - g_{21}^e n^m - g_{22}^e p^m - \sigma^p \Delta_h p^{m+1}. && (2.10)
\end{aligned}$$

Here, we have used a convex-concave decomposition of the symmetric matrix G

$$G = G_c - G_e, \tag{2.11}$$

in which both $G_c = (g_{i,j}^c)$ and $G_e = (g_{i,j}^e)$ are non-negative definite matrices. The mobility functions at the face-centered mesh points are defined as

$$\begin{aligned}
&(\check{\mathcal{M}}_n^m)_{i+\frac{1}{2},j,k} := \mathcal{A}_x (\mathcal{M}_n^m)_{i+\frac{1}{2},j,k}, \\
&(\check{\mathcal{M}}_n^m)_{i,j+\frac{1}{2},k} := \mathcal{A}_y (\mathcal{M}_n^m)_{i,j+\frac{1}{2},k}, \\
&(\check{\mathcal{M}}_n^m)_{i,j,k+\frac{1}{2}} := \mathcal{A}_z (\mathcal{M}_n^m)_{i,j,k+\frac{1}{2}},
\end{aligned} \tag{2.12}$$

in which $(\mathcal{M}_n^m)_{i,j,k} = n_{i,j,k}^m$, $(\mathcal{M}_p^m)_{i,j,k} = D p_{i,j,k}^m$. Similar definitions could be introduced for $\check{\mathcal{M}}_p^m$.

It is clear that the numerical solution to (2.7)-(2.10) is mass conservative, i.e.,

$$\overline{n^m} = \overline{n^0} := \beta_0, \quad \overline{p^m} = \overline{p^0} := \beta_0 \quad \text{with} \quad 0 < \beta_0, \quad \forall m \geq 1, \tag{2.13}$$

in which the average operator is given by $\overline{f} = (1/|\Omega|)\langle f, \mathbf{1}\rangle$. In addition, a few notations need to be introduced, to facilitate the analysis in later sections. For any $\varphi \in \mathring{\mathcal{C}}_{\rm per}$, the weighted discrete norm is defined as

$$\|\varphi\|_{\mathcal{L}^{-1}_{\check{\mathcal{M}}}} = \sqrt{\langle \varphi, \mathcal{L}^{-1}_{\check{\mathcal{M}}}(\varphi)\rangle}, \tag{2.14}$$

in which $\psi = \mathcal{L}^{-1}_{\check{\mathcal{M}}}(\varphi) \in \mathring{\mathcal{C}}_{\rm per}$ is the unique solution that solves

$$\mathcal{L}_{\check{\mathcal{M}}}(\psi) := -\nabla_h \cdot (\check{\mathcal{M}} \nabla_h \psi) = \varphi. \tag{2.15}$$

In a simplified case of $\check{\mathcal{M}} \equiv 1$, it is obvious that $\mathcal{L}_{\check{\mathcal{M}}}(\psi) = -\Delta_h \psi$, and the discrete H_h^{-1} norm is introduced as

$$\|\varphi\|_{-1,h} = \sqrt{\langle \varphi, (-\Delta_h)^{-1}(\varphi)\rangle}.$$

The positivity-preserving and unique solvability properties have been established in our recent work [43].

Theorem 2.1 ([43]). *Given $n^m, p^m \in \mathcal{C}_{\rm per}$, with $0 < n^m_{i,j,k}, p^m_{i,j,k}$, $1 \le i,j,k \le N$, and $n^m - p^m \in \mathring{\mathcal{C}}_{\rm per}$, there exists a unique solution $(n^{m+1}, p^{m+1}) \in [\mathcal{C}_{\rm per}]^2$ to the numerical scheme* (2.7)-(2.10)*, with $0 < n^{m+1}_{i,j,k}, p^{m+1}_{i,j,k}$, $1 \le i,j,k \le N$ and $n^{m+1} - p^{m+1} \in \mathring{\mathcal{C}}_{\rm per}$.*

The discrete energy is defined as

$$\begin{aligned} E_h(n,p) :=& \langle n \ln n + p \ln p, \mathbf{1}\rangle + \frac{1}{2}\|n-p\|^2_{-1,h} + \frac{1}{2}\big\langle (n,p), G(n,p)^T \big\rangle \\ &+ \frac{1}{2}\sigma^n \|\nabla_h n\|_2^2 + \frac{1}{2}\sigma^p \|\nabla_p p\|_2^2. \end{aligned} \tag{2.16}$$

Theorem 2.2 ([43]). *For the numerical solution* (2.7)-(2.10)*, we have*

$$\begin{aligned} &E_h(n^{m+1}, p^{m+1}) + \Delta t\Big(\Big[\check{\mathcal{M}}^m_n \nabla_h \mu_n^{m+1}, \nabla_h \mu_n^{m+1}\Big] + \Big[\check{\mathcal{M}}^m_p \nabla_h \mu_p^{m+1}, \nabla_h \mu_p^{m+1}\Big]\Big) \\ \le& E_h(n^m, p^m), \end{aligned} \tag{2.17}$$

so that $E_h(n^m, p^m) \le E_h(n^0, p^0) \le C_0$, for all $m \in \mathbb{N}$, where $C_0 > 0$ is a constant independent of h.

2.3 Main theoretical result: Optimal rate convergence analysis

Denote $(\mathsf{N}, \mathsf{P}, \Phi)$ as the exact PDE solution for the non-dimensional PNPCH system (1.1)-(1.3). We are able to assume a regularity of class $\mathcal{R}$ for the exact solution

$$\mathsf{N}, \mathsf{P} \in \mathcal{R} := H^4\big(0,T; C_{\rm per}(\Omega)\big) \cap H^3\big(0,T; C^2_{\rm per}(\Omega)\big) \cap L^\infty\big(0,T; C^8_{\rm per}(\Omega)\big), \tag{2.18}$$

if the initial data are regular enough. Moreover, the following separation property is assumed for the exact solution:

$$\mathsf{N} \ge \epsilon_0, \quad \mathsf{P} \ge \epsilon_0 \quad \text{for some} \quad \epsilon_0 > 0 \quad \text{at a point-wise level.} \tag{2.19}$$

Meanwhile, the Fourier projection of the exact solution is introduced

$$\mathsf{N}_N(\cdot,t) := \mathcal{P}_N \mathsf{N}(\cdot,t), \quad \mathsf{P}_N(\cdot,t) := \mathcal{P}_N \mathsf{P}(\cdot,t)$$

with the projection into $\mathcal{B}^K$, the space of trigonometric polynomials of degree to and including K (with $N=2K+1$). Subsequently, the projection approximation estimate is standard

$$\begin{aligned}&\|\mathsf{N}_N - \mathsf{N}\|_{L^\infty(0,T;H^k)} \le Ch^{\ell-k}\|\mathsf{N}\|_{L^\infty(0,T;H^\ell)},\\ &\|\mathsf{P}_N - \mathsf{P}\|_{L^\infty(0,T;H^k)} \le Ch^{\ell-k}\|\mathsf{P}\|_{L^\infty(0,T;H^\ell)}\end{aligned} \tag{2.20}$$

for any $0 \le k \le \ell$, provided that $(\mathsf{N},\mathsf{P}) \in L^\infty(0,T;H^\ell_{\rm per}(\Omega))$. In fact, the Fourier projection estimate (2.20) does not automatically ensure the positivity of the ion concentration variables; however, by taking h sufficiently small, a similar phase separation property is valid: $\mathsf{N}_N \ge (3/4)\epsilon_0$, $\mathsf{P}_N \ge (3/4)\epsilon_0$.

Meanwhile, a notation $\mathsf{N}_N^m = \mathsf{N}_N(\cdot,t_m)$, $\mathsf{P}_N^m = \mathsf{P}_N(\cdot,t_m)$ (with $t_m = m\cdot\Delta t$) is introduced, to facilitate the presentation. The mass conservative property is obvious at the discrete level

$$\begin{aligned}&\overline{\mathsf{N}_N^m} = \frac{1}{|\Omega|}\int_\Omega \mathsf{N}_N(\cdot,t_m)\,d\mathbf{x} = \frac{1}{|\Omega|}\int_\Omega \mathsf{N}_N(\cdot,t_{m-1})\,d\mathbf{x} = \overline{\mathsf{N}_N^{m-1}},\\ &\overline{\mathsf{P}_N^m} = \overline{\mathsf{P}_N^{m-1}}, \quad \forall m \in \mathbb{N}, \quad \text{(similar analysis)},\end{aligned} \tag{2.21}$$

due to the fact that $(\mathsf{N}_N,\mathsf{P}_N) \in \mathcal{B}^K$. On the other hand, the mass conservative identity (2.13) of the numerical solution (2.7)-(2.8) is recalled. In turn, the following point-wise interpolation is taken for the initial data in the numerical solution:

$$(n^0)_{i,j,k} := \mathsf{N}_N(p_i,p_j,p_k,t=0), \quad (p^0)_{i,j,k} := \mathsf{P}_N(p_i,p_j,p_k,t=0). \tag{2.22}$$

For the exact electric potential Φ, we denote its Fourier projection as Φ_N. Subsequently, the following definition is introduced for the error grid function:

$$e_n^m := \mathcal{P}_h \mathsf{N}_N^m - n^m, \quad e_p^m := \mathcal{P}_h \mathsf{P}_N^m - p^m, \quad e_\phi^m := \mathcal{P}_h \Phi_N^m - \phi^m, \quad \forall m \in \mathbb{N}. \tag{2.23}$$

The above analysis implies that $\overline{e_n^m} = \overline{e_p^m} = 0$ for any $m \in \mathbb{N}$.

The following theorem is the main result of this article.

Theorem 2.3. *Given initial data* $\mathsf{N}(\cdot,t=0),\mathsf{P}(\cdot,t=0) \in C^6_{\rm per}(\Omega)$, *suppose the exact solution for the PNPCH system* (1.1)-(1.2) *is of regularity class* $\mathcal{R}$. *Then, provided* Δt *and* h *are sufficiently small, and under the linear refinement requirement* $C_1 h \le \Delta t \le C_2 h$, *we have*

$$\|e_n^m\|_2 + \|e_p^m\|_2 + \left(\Delta t \sum_{k=1}^m \left(\|\Delta_h e_n^k\|_2^2 + \|\Delta_h e_p^k\|_2^2\right)\right)^{\frac{1}{2}} + \|e_\phi^m\|_{H_h^2} \le C(\Delta t + h^2) \tag{2.24}$$

for all positive integers m, *such that* $t_m = m\Delta t \le T$, *where* C_1, C_2, *and* C *are positive constants independent of* Δt *and* h.

3 Higher order consistency analysis of (2.7)-(2.10): Asymptotic expansion of the numerical solution

The Taylor expansion in both time and space indicates a first order temporal accuracy in time and second order spatial accuracy for the discrete equations (2.7)-(2.10), with a substitution of the project solution N_N, P_N. However, such a leading local truncation error will not be sufficient to recover an a priori ℓ^∞ bound for the numerical solution to establish the separation property. To deal with this theoretical challenge, we have to perform a higher order consistency analysis, with the help of linearization technique, which would be sufficient to derive such a bound in later analysis. In more details, we construct two supplementary fields, namely $\mathsf{N}_{\Delta t,1}$, $\mathsf{P}_{\Delta t,1}$, and define the following profiles:

$$\hat{\mathsf{N}}=\mathsf{N}_N+\Delta t\mathcal{P}_N\mathsf{N}_{\Delta t,1},\quad \hat{\mathsf{P}}=\mathsf{P}_N+\Delta t\mathcal{P}_N\mathsf{P}_{\Delta t,1}. \tag{3.1}$$

In fact, a higher $\mathcal{O}(\Delta t^2+h^2)$ consistency is satisfied with the given numerical scheme (2.7)-(2.10). The constructed profiles, $\mathsf{N}_{\Delta t,1}$ and $\mathsf{P}_{\Delta t,1}$, $\mathsf{P}_{h,1}$ will depend solely on the exact solution (N,P). In other words, a higher order approximate expansion of the exact solution is introduced to overcome the difficulty that a leading order consistency estimate is not able to control the ℓ^∞ norm of the numerical solution. Instead of substituting the exact solution into the numerical scheme, a careful construction of an approximate profile is performed by adding $\mathcal{O}(\Delta t)$ correction terms, so that an $\mathcal{O}(\Delta t^2+h^2)$ truncation error is satisfied. In turn, we estimate the numerical error function between the constructed profile and the numerical solution, instead of a direct comparison between the numerical solution and exact solution. Such a higher order consistency enables one to derive a higher order convergence estimate in the $\|\cdot\|_2$ norm, which in turn leads to the ℓ^∞ and $\|\cdot\|_{W_h^{1,4}}$ bounds of the numerical solution, via an application of inverse inequality. This approach has been reported for a wide class of nonlinear PDEs; see the related works for the incompressible fluid equation [16,17,45,46,52–54], various gradient equations [1,24,25,35], the porous medium equation based on the energetic variational approach [15], nonlinear wave equation [56], etc.

The following truncation error analysis for the temporal discretization can be obtained by using a straightforward Taylor expansion in time, combined with the projection estimate (2.20):

$$\begin{aligned}\frac{\mathsf{N}_N^{m+1}-\mathsf{N}_N^m}{\Delta t}=&\nabla\cdot\Big(\mathsf{N}_N^m\nabla\big(\ln\mathsf{N}_N^{m+1}+(-\Delta)^{-1}(\mathsf{N}_N^{m+1}-\mathsf{P}_N^{m+1})\big)+g_{11}^c\mathsf{N}_N^{m+1}\\&\qquad+g_{12}^c\mathsf{P}_N^{m+1}-g_{11}^e\mathsf{N}_N^m-g_{12}^e\mathsf{P}_N^m-\sigma^n\Delta_h\mathsf{N}_N^{m+1}\Big)\\&+\Delta t\big(G_n^{(0)}\big)^m+\mathcal{O}(\Delta t^2)+\mathcal{O}(h^{m_0}),\end{aligned}\tag{3.2}$$

$$\begin{aligned}\frac{\mathsf{P}_N^{m+1}-\mathsf{P}_N^m}{\Delta t}=&\nabla\cdot\Big(D\mathsf{P}_N^m\nabla\big(\ln\mathsf{P}_N^{m+1}+(-\Delta)^{-1}(\mathsf{P}_N^{m+1}-\mathsf{N}_N^{m+1})\big)+g_{21}^c\mathsf{N}_N^{m+1}\\&\qquad+g_{22}^c\mathsf{P}_N^{m+1}-g_{21}^e\mathsf{N}_N^m-g_{22}^e\mathsf{P}_N^m-\sigma^p\Delta_h\mathsf{P}_N^{m+1}\Big)\end{aligned}$$

$$+\Delta t\big(G_p^{(0)}\big)^m+\mathcal{O}(\Delta t^2)+\mathcal{O}(h^{m_0}). \tag{3.3}$$

The spectral accuracy order is given by $m_0\geq 4$, and the spatial functions $G_n^{(0)}$, $G_p^{(0)}$ are smooth enough in the sense that their derivatives are bounded.

Subsequently, the leading order temporal correction function $(\mathsf{N}_{\Delta t,1},\mathsf{P}_{\Delta t,1})$ turns out to be the following equations:

$$\begin{aligned}\partial_t\mathsf{N}_{\Delta t,1}=\nabla\cdot\Big(&\mathsf{N}_{\Delta t,1}\nabla\Big(\ln\mathsf{N}_N+(-\Delta)^{-1}(\mathsf{N}_N-\mathsf{P}_N)+g_{11}\mathsf{N}_N+g_{12}\mathsf{P}_N-\sigma^n\Delta\mathsf{N}_N\Big)\\&+\mathsf{N}_N\nabla\Big(\frac{1}{\mathsf{N}_N}\mathsf{N}_{\Delta t,1}+(-\Delta)^{-1}\big(\mathsf{N}_{\Delta t,1}-\mathsf{P}_{\Delta t,1}\big)\Big)\\&+\mathsf{N}_N\nabla\big(g_{11}\mathsf{N}_{\Delta t,1}+g_{12}\mathsf{P}_{\Delta t,1}-\sigma^n\Delta\mathsf{N}_{\Delta t,1}\big)\Big)-G_n^{(0)},\end{aligned} \tag{3.4}$$

$$\begin{aligned}\partial_t\mathsf{P}_{\Delta t,1}=\nabla\cdot\Big(&D\mathsf{P}_{\Delta t,1}\nabla\Big(\ln\mathsf{P}_N+(-\Delta)^{-1}(\mathsf{P}_N-\mathsf{N}_N)+g_{21}\mathsf{N}_N+g_{22}\mathsf{P}_N-\sigma^n\Delta\mathsf{P}_N\Big)\\&+D\mathsf{P}_N\nabla\Big(\frac{1}{\mathsf{P}_N}\mathsf{P}_{\Delta t,1}+(-\Delta)^{-1}\big(\mathsf{P}_{\Delta t,1}-\mathsf{N}_{\Delta t,1}\big)\Big)\\&+D\mathsf{P}_N\nabla\big(g_{21}\mathsf{N}_{\Delta t,1}+g_{22}\mathsf{P}_{\Delta t,1}-\sigma^p\Delta\mathsf{P}_{\Delta t,1}\big)\Big)-G_p^{(0)}.\end{aligned} \tag{3.5}$$

Existence of a solution of the above linear PDE system is straightforward; see the related textbook reference [51]. In fact, the solution depends only on the projection solution $(\mathsf{N}_N,\mathsf{P}_N)$, and the derivatives of $(\mathsf{N}_{\Delta t,1},\mathsf{P}_{\Delta t,1})$ are bounded in various orders. Also, trivial initial data $\mathsf{N}_{\Delta t,1}(\cdot,t=0)$, $\mathsf{P}_{\Delta t,1}(\cdot,t=0)\equiv 0$ could be imposed in (3.4)-(3.5). As a result, the mass conservative property is valid for $(\mathsf{N}_{\Delta t,1},\mathsf{P}_{\Delta t,1})$

$$\overline{\mathsf{N}_{\Delta t,1}(\cdot,t^k)}=\overline{\mathsf{P}_{\Delta t,1}(\cdot,t^k)}=0,\quad\forall k\geq 0. \tag{3.6}$$

An application of the semi-implicit discretization (as given by (3.2)-(3.3)) to (3.4)-(3.5) implies that

$$\begin{aligned}\frac{\mathsf{N}_{\Delta t,1}^{m+1}-\mathsf{N}_{\Delta t,1}^m}{\Delta t}=\nabla\cdot\Big(&\mathsf{N}_{\Delta t,1}^m\nabla\Big(\ln\mathsf{N}_N^{m+1}+(-\Delta)^{-1}\big(\mathsf{N}_N^{m+1}-\mathsf{P}_N^{m+1}\big)\Big)\\&+\mathsf{N}_{\Delta t,1}^m\nabla\Big(g_{11}^c\mathsf{N}_N^{m+1}+g_{12}^c\mathsf{P}_N^{m+1}-g_{11}^e\mathsf{N}_N^m-g_{12}^e\mathsf{P}_N^m-\sigma^n\Delta\mathsf{N}_N^{m+1}\Big)\\&+\mathsf{N}_N^m\nabla\Big(\frac{1}{\mathsf{N}_N^{m+1}}\mathsf{N}_{\Delta t,1}^{m+1}+(-\Delta)^{-1}\big(\mathsf{N}_{\Delta t,1}^{m+1}-\mathsf{P}_{\Delta t,1}^{m+1}\big)\Big)\\&+\mathsf{N}_N^m\nabla\Big(g_{11}^c\mathsf{N}_{\Delta t,1}^{m+1}+g_{12}^c\mathsf{P}_{\Delta t,1}^{m+1}-g_{11}^e\mathsf{N}_{\Delta t,1}^m-g_{12}^e\mathsf{P}_{\Delta t,1}^m-\sigma^n\Delta\mathsf{N}_{\Delta t,1}^{m+1}\Big)\Big)\\&-\big(G_n^{(0)}\big)^m+\Delta t\boldsymbol{h}_1^m+\mathcal{O}(\Delta t^2),\end{aligned} \tag{3.7}$$

$$\begin{aligned}\frac{\mathsf{P}_{\Delta t,1}^{m+1}-\mathsf{P}_{\Delta t,1}^{m}}{\Delta t}=&\nabla\cdot\Bigg(D\mathsf{P}_{\Delta t,1}^{m}\nabla\left(\ln\mathsf{P}_N^{m+1}+(-\Delta)^{-1}\big(\mathsf{P}_N^{m+1}-\mathsf{N}_N^{m+1}\big)\right)\\&+D\mathsf{P}_{\Delta t,1}^{m}\nabla\left(g_{21}^{c}\mathsf{N}_N^{m+1}+g_{22}^{c}\mathsf{P}_N^{m+1}-g_{21}^{e}\mathsf{N}_N^{m}-g_{22}^{e}\mathsf{P}_N^{m}-\sigma^p\Delta\mathsf{P}_N^{m+1}\right)\\&+D(\mathsf{P}_N)^m\nabla\left(\frac{1}{\mathsf{P}_N^{m+1}}\mathsf{P}_{\Delta t,1}^{m+1}+(-\Delta)^{-1}\big(\mathsf{P}_{\Delta t,1}^{m+1}-\mathsf{N}_{\Delta t,1}^{m+1}\big)\right)\\&+D(\mathsf{P}_N)^m\nabla\left(g_{21}^{c}\mathsf{N}_{\Delta t,1}^{m+1}+g_{22}^{c}\mathsf{P}_{\Delta t,1}^{m+1}-g_{21}^{e}\mathsf{N}_{\Delta t,1}^{m}-g_{22}^{e}\mathsf{P}_{\Delta t,1}^{m}-\sigma^p\Delta\mathsf{P}_{\Delta t,1}^{m+1}\right)\Bigg)\\&-\big(G_p^{(0)}\big)^m+\Delta t\boldsymbol{h}_2^m+\mathcal{O}(\Delta t^2).\end{aligned}\tag{3.8}$$

Consequently, a combination of (3.2)-(3.3) and (3.7)-(3.8) leads to the second order temporal truncation error for $\hat{\mathsf{N}}_1:=\mathsf{N}_N+\Delta t\mathcal{P}_N\mathsf{N}_{\Delta t,1}$, $\hat{\mathsf{P}}_1:=\mathsf{P}_N+\Delta t\mathcal{P}_N\mathsf{P}_{\Delta t,1}$

$$\begin{aligned}\frac{\hat{\mathsf{N}}_1^{m+1}-\hat{\mathsf{N}}_1^{m}}{\Delta t}=&\nabla\cdot\Bigg(\hat{\mathsf{N}}_1^{m}\nabla\left(\ln\hat{\mathsf{N}}_1^{m+1}+(-\Delta)^{-1}\big(\hat{\mathsf{N}}_1^{m+1}-\hat{\mathsf{P}}_1^{m+1}\big)\right)\\&+\hat{\mathsf{N}}_1^{m}\nabla\left(g_{11}^{c}\hat{\mathsf{N}}_1^{m+1}+g_{12}^{c}\hat{\mathsf{P}}_1^{m+1}-g_{11}^{e}\hat{\mathsf{N}}_1^{m}-g_{12}^{e}\hat{\mathsf{P}}_1^{m}-\sigma^n\Delta\hat{\mathsf{N}}_1^{m+1}\right)\Bigg)\\&+\mathcal{O}(\Delta t^2)+\mathcal{O}(h^{m_0}),\end{aligned}\tag{3.9}$$

$$\begin{aligned}\frac{\hat{\mathsf{P}}_1^{m+1}-\hat{\mathsf{P}}_1^{m}}{\Delta t}=&\nabla\cdot\Bigg(D\hat{\mathsf{P}}_1^{m}\nabla\left(\ln\hat{\mathsf{P}}_1^{m+1}+(-\Delta)^{-1}\big(\hat{\mathsf{P}}_1^{m+1}-\hat{\mathsf{N}}_1^{m+1}\big)\right)\\&+D\hat{\mathsf{P}}_1^{m}\nabla\left(g_{21}^{c}\hat{\mathsf{N}}_1^{m+1}+g_{22}^{c}\hat{\mathsf{P}}_1^{m+1}-g_{21}^{e}\hat{\mathsf{N}}_1^{m}-g_{22}^{e}\hat{\mathsf{P}}_1^{m}-\sigma^p\Delta\hat{\mathsf{P}}_1^{m+1}\right)\Bigg)\\&+\mathcal{O}(\Delta t^2)+\mathcal{O}(h^{m_0}).\end{aligned}\tag{3.10}$$

In the derivation of (3.9)-(3.10), the following linearized expansions have been utilized:

$$\ln\hat{\mathsf{N}}_1=\ln(\mathsf{N}_N+\Delta t\mathcal{P}_N\mathsf{N}_{\Delta t,1})=\ln\mathsf{N}_N+\frac{\Delta t\mathcal{P}_N\mathsf{N}_{\Delta t,1}}{\mathsf{N}_N}+\mathcal{O}(\Delta t^2),\tag{3.11}$$

$$\ln\hat{\mathsf{P}}_1=\ln(\mathsf{P}_N+\Delta t\mathcal{P}_N\mathsf{P}_{\Delta t,1})=\ln\mathsf{P}_N+\frac{\Delta t\mathcal{P}_N\mathsf{P}_{\Delta t,1}}{\mathsf{P}_N}+\mathcal{O}(\Delta t^2).\tag{3.12}$$

Furthermore, an application of finite difference approximation, combined with the Taylor expansion in space, yields the truncation error for $(\hat{\mathsf{N}},\hat{\mathsf{P}})$ (as given by (3.1))

$$\begin{aligned}\frac{\hat{\mathsf{N}}^{m+1}-\hat{\mathsf{N}}^{m}}{\Delta t}=&\nabla_h\cdot\Big(\mathcal{A}(\hat{\mathsf{N}}^m)\nabla_h\Big(\ln\hat{\mathsf{N}}^{m+1}+(-\Delta_h)^{-1}\big(\hat{\mathsf{N}}^{m+1}-\hat{\mathsf{P}}^{m+1}\big)+g_{11}^{c}\hat{\mathsf{N}}^{m+1}\\&+g_{12}^{c}\hat{\mathsf{P}}^{m+1}-g_{11}^{e}\hat{\mathsf{N}}^{m}-g_{12}^{e}\hat{\mathsf{P}}^{m}-\sigma^n\Delta_h\hat{\mathsf{N}}^{m+1}\Big)\Big)+\tau_n^{m+1},\end{aligned}\tag{3.13}$$

$$\frac{\hat{\mathsf{P}}^{m+1}-\hat{\mathsf{P}}^{m}}{\Delta t}=\nabla_h\cdot\Big(D\mathcal{A}(\hat{\mathsf{P}}^m)\nabla_h\Big(\ln\hat{\mathsf{P}}^{m+1}+(-\Delta_h)^{-1}\big(\hat{\mathsf{P}}^{m+1}-\hat{\mathsf{N}}^{m+1}\big)+g_{21}^{c}\hat{\mathsf{N}}^{m+1}$$

$$+g_{22}^{c}\hat{\mathsf{P}}^{m+1}-g_{21}^{e}\hat{\mathsf{N}}^{m}-g_{22}^{e}\hat{\mathsf{P}}^{m}-\sigma^{p}\Delta_h\hat{\mathsf{P}}^{m+1}\Big)\Big)+\tau_p^{m+1}, \tag{3.14}$$

where

$$\|\tau_n^{m+1}\|_2, \|\tau_p^{m+1}\|_2 \le C(\Delta t^2+h^2).$$

Based on the mass conservative property (3.6), combined with similar arguments as in (2.21), we conclude that

$$n^0\equiv\hat{\mathsf{N}}^0, \quad p^0\equiv\hat{\mathsf{P}}^0, \quad \overline{n^k}=\overline{n^0}, \quad \overline{p^k}=\overline{p^0}, \qquad \forall k\ge 0, \tag{3.15}$$

$$\overline{\hat{\mathsf{N}}^k}=\frac{1}{|\Omega|}\int_\Omega \hat{\mathsf{N}}(\cdot,t_k)d\mathbf{x}=\frac{1}{|\Omega|}\int_\Omega \hat{\mathsf{N}}^0 d\mathbf{x}=\overline{n^0}, \quad \overline{\hat{\mathsf{P}}^k}=\overline{p^0}, \quad \forall k\ge 0. \tag{3.16}$$

In addition, since $(\hat{\mathsf{N}},\hat{\mathsf{P}})$ is mass conservative at a discrete level, we see that the local truncation error τ_n and τ_p have a similar property

$$\overline{\tau_n^{m+1}}=\overline{\tau_p^{m+1}}=0, \quad \forall m\ge 0. \tag{3.17}$$

As another important feature, it is observed that the temporal correction functions $(\mathsf{N}_{\Delta t,1},\mathsf{P}_{\Delta t,1})$ are point-wise bounded. A combination of this fact with the separation property (2.19) (for the exact solution) leads to a similar lower bound for the constructed profile $(\hat{\mathsf{N}},\hat{\mathsf{P}})$

$$\hat{\mathsf{N}}\ge\epsilon_0^\star, \quad \hat{\mathsf{P}}\ge\epsilon_0^\star \quad \text{for} \quad \epsilon_0^\star=\frac{1}{2}\epsilon_0>0, \tag{3.18}$$

provided that Δt and h are sufficiently small, in which the projection estimate (2.20) has been repeatedly used. This uniform bound will be used in the convergence analysis. In addition, since the correction functions only depend on $(\mathsf{N}_N,\mathsf{P}_N)$ and the exact solution, its $W^{1,\infty}$ norm will stay bounded. In turn, we are able to obtain a discrete $W^{1,\infty}$ bound for the constructed profile $(\hat{\mathsf{N}},\hat{\mathsf{P}})$

$$\|\hat{\mathsf{N}}^k\|_\infty\le C^\star, \quad \|\hat{\mathsf{P}}^k\|_\infty\le C^\star, \quad \|\nabla_h\hat{\mathsf{N}}^k\|_\infty\le C^\star, \quad \|\nabla_h\hat{\mathsf{P}}^k\|_\infty\le C^\star, \quad \forall k\ge 0. \tag{3.19}$$

The reason for such a higher order asymptotic expansion and truncation error estimate is to justify an a priori ℓ^∞ bound of the numerical solution, which is needed to obtain the separation property, similarly formulated as (3.18) for the constructed approximate solution. With such a property valid for both the constructed approximate solution and the numerical solution, the nonlinear error term could be appropriately analyzed in the $\ell^\infty(0,T;\ell^2)$ convergence estimate.

4 A rough error estimate

Instead of a direct analysis for the error function defined in (2.23), we introduce alternate numerical error functions

$$\tilde{n}^m:=\mathcal{P}_h\hat{\mathsf{N}}^m-n^m, \quad \tilde{p}^m:=\mathcal{P}_h\hat{\mathsf{P}}^m-p^m, \quad \tilde{\phi}^m:=(-\Delta_h)^{-1}(\tilde{p}^m-\tilde{n}^m), \quad \forall m\in\mathbb{N}. \tag{4.1}$$

The advantage of such a numerical error function is associated with its higher order accuracy, which comes from the higher order consistency estimate (3.13)-(3.14). Because of the fact that $\overline{\tilde{n}^m}=\overline{\tilde{p}^m}=0$, for any $m\geq 0$ (which comes from the identities (3.15)-(3.16)), it is clear that the discrete norm $\|\cdot\|_{-1,h}$ is well defined for the error grid function $(\tilde{n}^m,\tilde{p}^m)$. In turn, subtracting the numerical scheme (2.7)-(2.10) from the consistency estimate (3.13)-(3.14) gives

$$\frac{\tilde{n}^{m+1}-\tilde{n}^m}{\Delta t}=\nabla_h\cdot\left(n^m\nabla_h\tilde{\mu}_n^{m+1}+\tilde{n}^m\nabla_h\mathcal{V}_n^{m+1}\right)+\tau_n^{m+1}, \tag{4.2}$$

$$\frac{\tilde{p}^{m+1}-\tilde{p}^m}{\Delta t}=\nabla_h\cdot\left(Dp^m\nabla_h\tilde{\mu}_p^{m+1}+D\tilde{p}^m\nabla_h\mathcal{V}_p^{m+1}\right)+\tau_p^{m+1} \tag{4.3}$$

with the following expansions:

$$\begin{aligned}\tilde{\mu}_n^{m+1}=&\ln\hat{\mathsf{N}}^{m+1}-\ln n^{m+1}+(-\Delta_h)^{-1}(\tilde{n}^{m+1}-\tilde{p}^{m+1})+g_{11}^c\tilde{n}^{m+1}\\&+g_{12}^c\tilde{p}^{m+1}-g_{11}^e\tilde{n}^m-g_{12}^c\tilde{p}^m-\sigma^n\Delta_h\tilde{n}^{m+1},\end{aligned} \tag{4.4}$$

$$\begin{aligned}\mathcal{V}_n^{m+1}=&\ln\hat{\mathsf{N}}^{m+1}+(-\Delta_h)^{-1}(\hat{\mathsf{N}}^{m+1}-\hat{\mathsf{P}}^{m+1})+g_{11}^c\hat{\mathsf{N}}^{m+1}\\&+g_{12}^c\hat{\mathsf{P}}^{m+1}-g_{11}^e\hat{\mathsf{N}}^m-g_{12}^c\hat{\mathsf{P}}^m-\sigma^n\Delta_h\hat{\mathsf{N}}^{m+1},\end{aligned} \tag{4.5}$$

$$\begin{aligned}\tilde{\mu}_p^{m+1}=&\ln\hat{\mathsf{P}}^{m+1}-\ln p^{m+1}+(-\Delta_h)^{-1}(\tilde{p}^{m+1}-\tilde{n}^{m+1})+g_{21}^c\tilde{n}^{m+1}\\&+g_{22}^c\tilde{p}^{m+1}-g_{21}^e\tilde{n}^m-g_{22}^c\tilde{p}^m-\sigma^n\Delta_h\tilde{p}^{m+1},\end{aligned} \tag{4.6}$$

$$\begin{aligned}\mathcal{V}_p^{m+1}=&\ln\hat{\mathsf{P}}^{m+1}+(-\Delta_h)^{-1}(\hat{\mathsf{P}}^{m+1}-\hat{\mathsf{N}}^{m+1})+g_{21}^c\hat{\mathsf{N}}^{m+1}\\&+g_{22}^c\hat{\mathsf{P}}^{m+1}-g_{21}^e\hat{\mathsf{N}}^m-g_{22}^c\hat{\mathsf{P}}^m-\sigma^p\Delta_h\hat{\mathsf{P}}^{m+1}.\end{aligned} \tag{4.7}$$

Since $\mathcal{V}_n^{m+1}$ and $\mathcal{V}_p^{m+1}$ only depend on the exact solution and the constructed profiles, it is reasonable to assume a discrete $W^{1,\infty}$ bound

$$\|\mathcal{V}_n^{m+1}\|_{W_h^{1,\infty}},\ \|\mathcal{V}_p^{m+1}\|_{W_h^{1,\infty}}\leq C^\star. \tag{4.8}$$

In addition, to proceed with the nonlinear analysis, we make the following a priori assumption at the previous time step:

$$\|\tilde{n}^m\|_2+\|\tilde{p}^m\|_2\leq\Delta t^{\frac{15}{8}}+h^{\frac{15}{8}},\quad \|\Delta_h\tilde{n}^m\|_2+\|\Delta_h\tilde{p}^m\|_2\leq\Delta t^{\frac{11}{8}}+h^{\frac{11}{8}}. \tag{4.9}$$

This a priori assumption will be recovered by the optimal rate convergence analysis at the next time step, as will be proved later. In turn, a discrete ℓ^∞ and $W_h^{1,\infty}$ bound is available for the numerical error function at the previous time step, with the help of the discrete Sobolev inequality (2.5) (in Lemma 2.2), as well as the inverse inequality

$$\|\tilde{n}^m\|_\infty\leq C\left(\|\tilde{n}^m\|_2+\|\Delta_h\tilde{n}^m\|_2\right)\leq C\left(\Delta t^{\frac{11}{8}}+h^{\frac{11}{8}}\right)\leq\frac{1}{2}\epsilon_0^*\leq 1, \tag{4.10}$$

$$\|\nabla_h\tilde{n}^m\|_\infty\leq\frac{C\|\Delta_h\tilde{n}^m\|_2}{h^{\frac{1}{2}}}\leq\frac{C\left(\Delta t^{\frac{11}{8}}+h^{\frac{11}{8}}\right)}{h^{\frac{1}{2}}}\leq C\left(\Delta t^{\frac{7}{8}}+h^{\frac{7}{8}}\right)\leq 1, \tag{4.11}$$

where the linear refinement constraint $C_1 h \le \Delta t \le C_2 h$ has been used. A similar argument gives

$$\|\tilde{p}^m\|_\infty \le C\left(\Delta t^{\frac{11}{8}} + h^{\frac{11}{8}}\right) \le \frac{1}{2}\epsilon_0^* \le 1, \quad \|\nabla_h \tilde{p}^m\|_\infty \le C\left(\Delta t^{\frac{7}{8}} + h^{\frac{7}{8}}\right) \le 1. \tag{4.12}$$

Subsequently, the following $W_h^{1,\infty}$ bound is available for the numerical solution at the previous time step, combined with the regularity assumption (3.19):

$$\|n^m\|_\infty \le \|\hat{\mathsf{N}}^m\|_\infty + \|\tilde{n}^m\|_\infty \le \tilde{C}_3 := C^\star + 1, \qquad \|p^m\|_\infty \le \tilde{C}_3, \tag{4.13}$$

$$\|\nabla_h n^m\|_\infty \le \|\nabla_h \hat{\mathsf{N}}^m\|_\infty + \|\nabla_h \tilde{n}^m\|_\infty \le C^\star + 1 = \tilde{C}_3, \quad \|\nabla_h p^m\|_\infty \le = \tilde{C}_3. \tag{4.14}$$

As a further bound, a combination of the ℓ^∞ estimate (4.10), (4.12) for the numerical error function and the separation estimate (3.18) leads to a similar separation property for the numerical solution at the previous time step, at a point-wise level

$$n^m \ge \hat{\mathsf{N}}^m - \|\tilde{n}^m\|_\infty \ge \frac{\epsilon_0^\star}{2}, \quad p^m \ge \check{\mathsf{P}}^m - \|\tilde{p}^m\|_\infty \ge \frac{\epsilon_0^\star}{2}. \tag{4.15}$$

The following proposition states the rough error estimate result.

Proposition 4.1. *Under the regularity requirement assumption* (4.8) *for the constructed profiles* $\mathcal{V}_n^{m+1}$, $\mathcal{V}_p^{m+1}$, *as well as the a priori assumption* (4.9) *for the numerical solution at the previous time step, we have a rough error estimate*

$$\left\|\tilde{n}^{m+1}\right\|_2 + \left\|\nabla_h \tilde{n}^{m+1}\right\|_2 + \left\|\tilde{p}^{m+1}\right\|_2 + \left\|\nabla_h \tilde{p}^{m+1}\right\|_2 \le \Delta t^{\frac{5}{4}} + h^{\frac{5}{4}}. \tag{4.16}$$

Proof. Taking a discrete inner product with (4.2), (4.3) by $\tilde{\mu}_n^{n+1}$, $\tilde{\mu}_p^{n+1}$, respectively, gives

$$\begin{aligned}
&\left\langle \tilde{n}^{m+1}, \tilde{\mu}_n^{m+1} \right\rangle + \left\langle \tilde{p}^{m+1}, \tilde{\mu}_p^{m+1} \right\rangle \\
&\quad + \Delta t \Big(\left\langle \mathcal{A}(n^m) \nabla_h \tilde{\mu}_n^{m+1}, \nabla_h \tilde{\mu}_n^{m+1} \right\rangle + D \left\langle \mathcal{A}(p^m) \nabla_h \tilde{\mu}_p^{m+1}, \nabla_h \tilde{\mu}_p^{m+1} \right\rangle \Big) \\
&= \left\langle \tilde{n}^m, \tilde{\mu}_n^{m+1} \right\rangle + \left\langle \tilde{p}^m, \tilde{\mu}_p^{m+1} \right\rangle + \Delta t \Big(\left\langle \tau_n^{m+1}, \tilde{\mu}_n^{m+1} \right\rangle + \left\langle \tau_p^{m+1}, \tilde{\mu}_p^{m+1} \right\rangle \Big) \\
&\quad - \Delta t \Big(\left\langle \mathcal{A}(\tilde{n}^m) \nabla_h \mathcal{V}_n^{m+1}, \nabla_h \tilde{\mu}_n^{m+1} \right\rangle + D \left\langle \mathcal{A}(\tilde{p}^m) \nabla_h \mathcal{V}_p^{m+1}, \nabla_h \tilde{\mu}_p^{m+1} \right\rangle \Big).
\end{aligned} \tag{4.17}$$

In terms of the chemical potential diffusion terms, the following inequalities could be derived, based on the point-wise separation estimate (4.15):

$$\begin{aligned}
&\left\langle \mathcal{A}(n^m) \nabla_h \tilde{\mu}_n^{m+1}, \nabla_h \tilde{\mu}_n^{m+1} \right\rangle \ge \frac{\epsilon_0^\star}{2} \left\|\nabla_h \tilde{\mu}_n^{m+1}\right\|_2^2, \\
&\left\langle \mathcal{A}(p^m) \nabla_h \tilde{\mu}_p^{m+1}, \nabla_h \tilde{\mu}_p^{m+1} \right\rangle \ge \frac{\epsilon_0^\star}{2} \left\|\nabla_h \tilde{\mu}_p^{m+1}\right\|_2^2.
\end{aligned} \tag{4.18}$$

Since the local truncation error have zero mean, as given by (3.17), the following estimate are available:

$$\left\langle \tau_n^{m+1}, \tilde{\mu}_n^{m+1} \right\rangle \le \left\|\tau_n^{m+1}\right\|_{-1,h} \cdot \left\|\nabla_h \tilde{\mu}_n^{m+1}\right\|_2 \le \frac{2}{\epsilon_0^\star} \left\|\tau_n^{m+1}\right\|_{-1,h}^2 + \frac{1}{8}\epsilon_0^\star \left\|\nabla_h \tilde{\mu}_n^{m+1}\right\|_2^2, \tag{4.19}$$

$$\left\langle \tau_p^{m+1},\tilde{\mu}_p^{m+1}\right\rangle \le \left\|\tau_p^{m+1}\right\|_{-1,h}\cdot\left\|\nabla_h\tilde{\mu}_p^{m+1}\right\|_2 \le \frac{2}{D\epsilon_0^\star}\left\|\tau_p^{m+1}\right\|_{-1,h}^2+\frac{1}{8}D\epsilon_0^\star\left\|\nabla_h\tilde{\mu}_p^{m+1}\right\|_2^2. \tag{4.20}$$

Similarly, an application of the Cauchy inequality to $\langle\tilde{n}^m,\tilde{\mu}_n^{m+1}\rangle$ and $\langle\tilde{p}^m,\tilde{\mu}_p^{m+1}\rangle$ leads to

$$\left\langle \tilde{n}^m,\tilde{\mu}_n^{m+1}\right\rangle \le \left\|\tilde{n}^m\right\|_{-1,h}\cdot\left\|\nabla_h\tilde{\mu}_n^{m+1}\right\|_2 \le \frac{2}{\epsilon_0^\star\Delta t}\left\|\tilde{n}^m\right\|_{-1,h}^2+\frac{1}{8}\epsilon_0^\star\Delta t\left\|\nabla_h\tilde{\mu}_n^{m+1}\right\|_2^2, \tag{4.21}$$

$$\left\langle \tilde{p}^m,\tilde{\mu}_p^{m+1}\right\rangle \le \left\|\tilde{p}^m\right\|_{-1,h}\cdot\left\|\nabla_h\tilde{\mu}_p^{m+1}\right\|_2 \le \frac{2}{D\epsilon_0^\star\Delta t}\left\|\tilde{p}^m\right\|_{-1,h}^2+\frac{1}{8}D\epsilon_0^\star\Delta t\left\|\nabla_h\tilde{\mu}_p^{m+1}\right\|_2^2. \tag{4.22}$$

The last two terms on the right-hand side of (4.17) could be analyzed as follows:

$$\begin{aligned}
&-\left\langle \mathcal{A}(\tilde{n}^m)\nabla_h\mathcal{V}_n^{m+1},\nabla_h\tilde{\mu}_n^{m+1}\right\rangle\\
\le&\left\|\nabla_h\mathcal{V}_n^{m+1}\right\|_\infty\cdot\left\|\mathcal{A}(\tilde{n}^m)\right\|_2\cdot\left\|\nabla_h\tilde{\mu}_n^{m+1}\right\|_2\le C^\star\left\|\tilde{n}^m\right\|_2\cdot\left\|\nabla_h\tilde{\mu}_n^{m+1}\right\|_2\\
\le&\frac{2(C^\star)^2}{\epsilon_0^\star}\left\|\tilde{n}^m\right\|_2^2+\frac{1}{8}\epsilon_0^\star\left\|\nabla_h\tilde{\mu}_n^{m+1}\right\|_2^2,
\end{aligned}\tag{4.23}$$

$$-D\left\langle \mathcal{A}(\tilde{p}^m)\nabla_h\mathcal{V}_p^{m+1},\nabla_h\tilde{\mu}_p^{m+1}\right\rangle \le \frac{2(C^\star)^2D}{\epsilon_0^\star}\left\|\tilde{p}^m\right\|_2^2+\frac{1}{8}D\epsilon_0^\star\left\|\nabla_h\tilde{\mu}_p^{m+1}\right\|_2^2. \tag{4.24}$$

For the two terms $\langle\tilde{n}^{m+1},\tilde{\mu}_n^{m+1}\rangle$ and $\langle\tilde{p}^{m+1},\tilde{\mu}_p^{m+1}\rangle$, the detailed expansions in (4.4) and (4.6) indicate the following inequalities:

$$\left\langle \ln\hat{\mathsf{N}}^{m+1}-\ln n^{m+1},\tilde{n}^{m+1}\right\rangle=\left\langle \ln\hat{\mathsf{N}}^{m+1}-\ln n^{m+1},\hat{\mathsf{N}}^{m+1}-n^{m+1}\right\rangle\ge 0, \tag{4.25}$$

$$\left\langle \ln\hat{\mathsf{P}}^{m+1}-\ln p^{m+1},\tilde{p}^{m+1}\right\rangle=\left\langle \ln\hat{\mathsf{P}}^{m+1}-\ln p^{m+1},\hat{\mathsf{P}}^{m+1}-p^{m+1}\right\rangle\ge 0, \tag{4.26}$$

and

$$\begin{aligned}
&\left\langle(-\Delta_h)^{-1}(\tilde{n}^{m+1}-\tilde{p}^{m+1}),\tilde{n}^{m+1}\right\rangle+\left\langle(-\Delta_h)^{-1}(\tilde{p}^{m+1}-\tilde{n}^{m+1}),\tilde{p}^{m+1}\right\rangle\\
=&\left\|\tilde{n}^{m+1}-\tilde{p}^{m+1}\right\|_{-1,h}^2\ge 0,
\end{aligned}\tag{4.27}$$

$$\left\langle\tilde{n}^{m+1},-\Delta_h\tilde{n}^{m+1}\right\rangle=\left\|\nabla_h\tilde{n}^{m+1}\right\|_2^2,\quad \left\langle\tilde{p}^{m+1},-\Delta_h\tilde{p}^{m+1}\right\rangle=\left\|\nabla_h\tilde{p}^{m+1}\right\|_2^2, \tag{4.28}$$

$$\left\langle\tilde{n}^{m+1},g_{11}^c\tilde{n}^{m+1}+g_{12}^c\tilde{p}^{m+1}\right\rangle+\left\langle\tilde{p}^{m+1},g_{21}^c\tilde{n}^{m+1}+g_{22}^c\tilde{p}^{m+1}\right\rangle\ge 0, \tag{4.29}$$

$$\begin{aligned}
&-\left\langle\tilde{n}^{m+1},g_{11}^e\tilde{n}^m+g_{12}^e\tilde{p}^m\right\rangle\\
\ge&-\left\|\nabla_h\tilde{n}^{m+1}\right\|_2\cdot\left\|g_{11}^e\tilde{n}^m+g_{12}^e\tilde{p}^m\right\|_{-1,h}\\
\ge&-\frac{\sigma^n}{2}\left\|\nabla_h\tilde{n}^{m+1}\right\|_2^2-(\sigma^n)^{-1}\left((g_{11}^e)^2\left\|\tilde{n}^m\right\|_{-1,h}^2+(g_{12}^e)^2\left\|\tilde{p}^m\right\|_{-1,h}^2\right),
\end{aligned}\tag{4.30}$$

$$\begin{aligned}
&-\left\langle\tilde{p}^{m+1},g_{21}^e\tilde{n}^m+g_{22}^e\tilde{p}^m\right\rangle\\
\ge&-\left\|\nabla_h\tilde{p}^{m+1}\right\|_2\cdot\left\|g_{21}^e\tilde{n}^m+g_{22}^e\tilde{p}^m\right\|_{-1,h}\\
\ge&-\frac{\sigma^p}{2}\left\|\nabla_h\tilde{p}^{m+1}\right\|_2^2-(\sigma^p)^{-1}\left((g_{21}^e)^2\left\|\tilde{n}^m\right\|_{-1,h}^2+(g_{22}^e)^2\left\|\tilde{p}^m\right\|_{-1,h}^2\right),
\end{aligned}\tag{4.31}$$

where the positivities of (n^{m+1},p^{m+1}) and $(\check{\mathsf{N}}^{m+1},\check{\mathsf{P}}^{m+1})$ have been applied in the derivation of (4.25) and (4.26), as well as the application of positive-definite property of G^c in the derivation of (4.29). Then we conclude that

$$\begin{aligned}&\langle \tilde{n}^{m+1},\tilde{\mu}_n^{m+1}\rangle+\langle \tilde{p}^{m+1},\tilde{\mu}_p^{m+1}\rangle\\ \geq& \frac{\sigma^n}{2}\|\nabla_h\tilde{n}^{m+1}\|_2^2+\frac{\sigma^p}{2}\|\nabla_h\tilde{p}^{m+1}\|_2^2-Q_0\left(\|\tilde{n}^m\|_{-1,h}^2+\|\tilde{p}^m\|_{-1,h}^2\right)\end{aligned} \tag{4.32}$$

with

$$Q_0=\max\Big((\sigma^n)^{-1}(g_{11}^e)^2+(\sigma^p)^{-1}(g_{21}^e)^2,(\sigma^n)^{-1}(g_{12}^e)^2+(\sigma^p)^{-1}(g_{22}^e)^2\Big).$$

Therefore, a substitution of (4.18)-(4.24) and (4.32) into (4.17) reveals that

$$\begin{aligned}&\frac{\epsilon_0^\star}{2}\Delta t\Big(\|\nabla_h\tilde{\mu}_n^{m+1}\|_2^2+D\|\nabla_h\tilde{\mu}_p^{m+1}\|_2^2\Big)+\frac{\sigma^n}{2}\|\nabla_h\tilde{n}^{m+1}\|_2^2+\frac{\sigma^p}{2}\|\nabla_h\tilde{p}^{m+1}\|_2^2\\ \leq&\left(\frac{2}{\epsilon_0^\star\Delta t}+Q_0\right)\|\tilde{n}^m\|_{-1,h}^2+\left(\frac{2}{D\epsilon_0^\star\Delta t}+Q_0\right)\|\tilde{p}^m\|_{-1,h}^2+\frac{2\Delta t}{\epsilon_0^\star}\|\tau_n^{m+1}\|_{-1,h}^2\\ &+\frac{2\Delta t}{D\epsilon_0^\star}\|\tau_p^{m+1}\|_{-1,h}^2+2(C^\star)^2(\epsilon_0^\star)^{-1}\Delta t\Big(\|\tilde{n}^m\|_2^2+D^{-1}\|\tilde{p}^m\|_2^2\Big).\end{aligned} \tag{4.33}$$

The right-hand side of (4.33) could be bounded in the following manner, based on the a priori assumption (4.9):

$$\left(\frac{2}{\epsilon_0^\star\Delta t}+Q_0\right)\|\tilde{n}^m\|_{-1,h}^2\leq\frac{C}{\epsilon_0^\star\Delta t}\|\tilde{n}^m\|_2^2\leq C\Big(\Delta t^{\frac{11}{4}}+h^{\frac{11}{4}}\Big), \tag{4.34}$$

$$\left(\frac{2}{D\epsilon_0^\star\Delta t}+Q_0\right)\|\tilde{p}^m\|_{-1,h}^2\leq\frac{C}{D\epsilon_0^\star\Delta t}\|\tilde{p}^m\|_2^2\leq C\Big(\Delta t^{\frac{11}{4}}+h^{\frac{11}{4}}\Big), \tag{4.35}$$

$$\frac{2\Delta t}{\epsilon_0^\star}\|\tau_n^{m+1}\|_{-1,h}^2+\frac{2\Delta t}{D\epsilon_0^\star}\|\tau_p^{m+1}\|_{-1,h}^2\leq C\Delta t\Big(\|\tau_n^{m+1}\|_2^2+\|\tau_p^{m+1}\|_2^2\Big)\leq C\Delta t(\Delta t^4+h^4), \tag{4.36}$$

$$2(C^\star)^2(\epsilon_0^\star)^{-1}\Delta t\Big(\|\tilde{n}^m\|_2^2+D^{-1}\|\tilde{p}^m\|_2^2\Big)\leq C\Delta t\Big(\|\tilde{n}^m\|_2^2+\|\tilde{n}^m\|_2^2\Big)\leq C\Big(\Delta t^{\frac{19}{4}}+h^{\frac{19}{4}}\Big), \tag{4.37}$$

where the fact that $\|f\|_{-1,h}\leq C\|f\|_2$, as well as the linear refinement constraint $C_1h\leq\Delta t\leq C_2h$, have been repeatedly applied. Going back to (4.33), we arrive at

$$\frac{\sigma^n}{2}\|\nabla_h\tilde{n}^{m+1}\|_2^2+\frac{\sigma^p}{2}\|\nabla_h\tilde{p}^{m+1}\|_2^2\leq C\Big(\Delta t^{\frac{11}{4}}+h^{\frac{11}{4}}\Big). \tag{4.38}$$

This in turn reveals that

$$\|\tilde{n}^{m+1}\|_2+\|\nabla_h\tilde{n}^{m+1}\|_2+\|\tilde{p}^{m+1}\|_2+\|\nabla_h\tilde{p}^{m+1}\|_2\leq C\Big(\Delta t^{\frac{11}{8}}+h^{\frac{11}{8}}\Big)\leq\Delta t^{\frac{5}{4}}+h^{\frac{5}{4}}, \tag{4.39}$$

provided that Δt and h are sufficiently small, and the discrete Poincaré inequality (2.6) has been applied. This inequality is exactly the rough error estimate (4.16). The proof of Proposition 4.1 is finished. □

As a direct consequence of the rough error estimate (4.16), an application of 3D inverse inequality leads to

$$\begin{aligned}\|\tilde{n}^{m+1}\|_\infty+\|\tilde{p}^{m+1}\|_\infty &\le \frac{1}{h^{\frac{1}{2}}}C\Big(\|\tilde{n}^{m+1}\|_2+\|\nabla_h\tilde{n}^{m+1}\|_2+\|\tilde{p}^{m+1}\|_2+\|\nabla_h\tilde{p}^{m+1}\|_2\Big)\\ &\le C\Big(\Delta t^{\frac{3}{4}}+h^{\frac{3}{4}}\Big)\le\frac{\epsilon_0^\star}{2}\end{aligned} \tag{4.40}$$

under the same linear refinement requirement, provided that Δt and h are sufficiently small. In turn, the following separation is valid for the numerical solution at time step t^{m+1}:

$$\frac{\epsilon_0^\star}{2}\le n^{m+1}\le C^\star+\frac{\epsilon_0^\star}{2}\le\tilde{C}_3,\quad \frac{\epsilon_0^\star}{2}\le p^{m+1}\le C^\star+\frac{\epsilon_0^\star}{2}\le\tilde{C}_3. \tag{4.41}$$

This uniform $\|\cdot\|_\infty$ bound will play a very important role in the refined error estimate.

Meanwhile, by the rough error estimate (4.16), an application of inverse inequality gives an $\|\cdot\|_8$ bound for $(\tilde{n}^{m+1},\tilde{p}^{m+1})$

$$\begin{aligned}&\|\nabla_h\tilde{n}^{m+1}\|_8\le\frac{C\|\nabla_h\tilde{n}^{m+1}\|_2}{h^{\frac{9}{8}}}\le\frac{C\big(\Delta t^{\frac{5}{4}}+h^{\frac{5}{4}}\big)}{h^{\frac{9}{8}}}\le 1,\\ &\|\nabla_h\tilde{p}^{m+1}\|_8\le 1,\quad \text{(similarly)},\end{aligned} \tag{4.42}$$

in which the linear refinement requirement $C_1h\le\Delta t\le C_2h$ has been applied. In turn, the following $\|\cdot\|_8$ bound becomes available for (n^{m+1},p^{m+1})

$$\begin{aligned}&\|\nabla_h n^{m+1}\|_8\le\|\nabla_h\hat{\mathsf{N}}^{m+1}\|_8+\|\nabla_h\tilde{n}^{m+1}\|_8\le C^*+1=\tilde{C}_3,\\ &\|\nabla_h p^{m+1}\|_8\le\|\nabla_h\hat{\mathsf{P}}^{m+1}\|_8+\|\nabla_h\tilde{p}^{m+1}\|_8\le C^*+1=\tilde{C}_3.\end{aligned} \tag{4.43}$$

5 A refined error estimate

The following preliminary results are needed in the refined analysis for the numerical error functions. The proof of Lemmas 5.1 and 5.2 has been modified from the version in [37]. We here present the rewritten proof of Lemma 5.1 in Appendix A and just cite the result of Lemma 5.2 in this article.

Lemma 5.1 ([37]). *Under the a priori $\|\cdot\|_\infty$ estimate* (4.13), (4.15) *for the numerical solution at the previous time step and the rough $\|\cdot\|_\infty$ estimate* (4.41) *for the one at the next time step, we have*

$$\begin{aligned}&\big\langle\mathcal{A}(n^m)\nabla_h(\ln\check{\mathsf{N}}^{m+1}-\ln n^{m+1}),\nabla_h\tilde{n}^{m+1}\big\rangle\\ &\ge\gamma_n^{(0)}\|\nabla_h\tilde{n}^{m+1}\|_2^2-M_n^{(0)}\|\tilde{n}^{m+1}\|_2^2-M_n^{(1)}h^8,\end{aligned} \tag{5.1}$$

$$\begin{aligned}&D\big\langle\mathcal{A}(p^m)\nabla_h(\ln\check{\mathsf{P}}^{m+1}-\ln p^{m+1}),\nabla_h\tilde{p}^{m+1}\big\rangle\\ &\ge\gamma_p^{(0)}\|\nabla_h\tilde{p}^{m+1}\|_2^2-M_p^{(0)}\|\tilde{p}^{m+1}\|_2^2-M_p^{(1)}h^8,\end{aligned} \tag{5.2}$$

where the constants $\gamma_n^{(0)},\gamma_p^{(0)},M_n^{(0)},M_p^{(0)},M_n^{(1)},M_p^{(1)}$ only depend on $\epsilon_0^\star,C^\star,\tilde{C}_3,D$ and $|\Omega|$.

Lemma 5.2 ([37]). *For $\tilde{\phi}^k$ (for any $k\geq 0$) defined in* (4.1), *we have the estimate*

$$\|\nabla_h\tilde{\phi}^k\|_2 \leq \tilde{C}_4\|\tilde{n}^k-\tilde{p}^k\|_2 \tag{5.3}$$

for some constant $\tilde{C}_4>0$ that is independent of h.

Lemma 5.3. *Under the a priori $\|\cdot\|_\infty$ estimates* (4.13)-(4.14), (4.15) *for the numerical solution at the previous time step, we have*

$$-\sigma^n\langle\mathcal{A}(n^m)\nabla_h\Delta_h\tilde{n}^{m+1},\nabla_h\tilde{n}^{m+1}\rangle \geq \gamma_n^{(1)}\|\Delta_h\tilde{n}^{m+1}\|_2^2 - M_n^{(2)}\|\nabla_h\tilde{n}^{m+1}\|_2^2, \tag{5.4}$$

$$-D\sigma^p\langle\mathcal{A}(p^m)\nabla_h\Delta_h p^{m+1},\nabla_h\tilde{p}^{m+1}\rangle \geq \gamma_p^{(1)}\|\nabla_h\tilde{p}^{m+1}\|_2^2 - M_p^{(2)}\|\nabla_h\tilde{p}^{m+1}\|_2^2, \tag{5.5}$$

where the constants $\gamma_n^{(1)}$, $\gamma_p^{(1)}$, $M_n^{(2)}$ and $M_p^{(2)}$ only depend on $\epsilon_0^\star$, $C^\star$, $\tilde{C}_3$, σ^n, σ^p, D and $|\Omega|$.

Proof. An application of summation by parts implies that

$$-\langle\mathcal{A}(n^m)\nabla_h\Delta_h\tilde{n}^{m+1},\nabla_h\tilde{n}^{m+1}\rangle = \langle\Delta_h\tilde{n}^{m+1},\nabla_h\cdot(\mathcal{A}(n^m)\nabla_h\tilde{n}^{m+1})\rangle. \tag{5.6}$$

Meanwhile, at a fixed grid point (i,j,k), a detailed finite difference expansion reveals that

$$\begin{aligned}\nabla_h\cdot(\mathcal{A}(n^m)\nabla_h\tilde{n}^{m+1})_{i,j,k} = {} & n^m_{i,j,k}\Delta_h\tilde{n}^{m+1}_{i,j,k} + \frac{1}{2}\Big(D_x n^m_{i+\frac{1}{2},j,k}D_x\tilde{n}^{m+1}_{i+\frac{1}{2},j,k} + D_x n^m_{i-\frac{1}{2},j,k}D_x\tilde{n}^{m+1}_{i-\frac{1}{2},j,k}\Big)\\ & + \frac{1}{2}\Big(D_y n^m_{i,j+\frac{1}{2},k}D_y\tilde{n}^{m+1}_{i,j+\frac{1}{2},k} + D_y n^m_{i,j-\frac{1}{2},k}D_y\tilde{n}^{m+1}_{i,j-\frac{1}{2},k}\Big)\\ & + \frac{1}{2}\Big(D_z n^m_{i,j,k+\frac{1}{2}}D_z\tilde{n}^{m+1}_{i,j,k+\frac{1}{2}} + D_z n^m_{i,j,k-\frac{1}{2}}D_z\tilde{n}^{m+1}_{i,j,k-\frac{1}{2}}\Big).\end{aligned} \tag{5.7}$$

Subsequently, an application of discrete Hölder inequality leads to

$$\begin{aligned} & -\sigma^n\langle\mathcal{A}(n^m)\nabla_h\Delta_h\tilde{n}^{m+1},\nabla_h\tilde{n}^{m+1}\rangle\\ = {} & \sigma^n\langle\Delta_h\tilde{n}^{m+1},\nabla_h\cdot(\mathcal{A}(n^m)\nabla_h\tilde{n}^{m+1})\rangle\\ \geq {} & \sigma^n\min(n^m)\cdot\|\Delta_h\tilde{n}^{m+1}\|_2^2 - \sigma^n\|\nabla_h n^m\|_\infty\cdot\|\nabla_h\tilde{n}^{m+1}\|_2\cdot\|\Delta_h\tilde{n}^{m+1}\|_2\\ \geq {} & \frac{\sigma^n\epsilon_0^*}{2}\|\Delta_h\tilde{n}^{m+1}\|_2^2 - \tilde{C}_3\sigma^n\|\nabla_h\tilde{n}^{m+1}\|_2\cdot\|\Delta_h\tilde{n}^{m+1}\|_2\\ \geq {} & \frac{\sigma^n\epsilon_0^*}{4}\|\Delta_h\tilde{n}^{m+1}\|_2^2 - \tilde{C}_3^2\sigma^n(\epsilon_0^*)^{-1}\|\nabla_h\tilde{n}^{m+1}\|_2^2,\end{aligned} \tag{5.8}$$

in which the $\|\cdot\|_\infty$ estimates (4.14) and the phase separation property (4.15) have been applied in the derivation. As a result, we have proved inequality (5.4), by setting

$$\gamma_n^{(1)} = \frac{\sigma^n\epsilon_0^*}{4}, \quad M_n^{(2)} = \tilde{C}_3^2\sigma^n(\epsilon_0^*)^{-1}.$$

Inequality (5.5) can be established in a similar manner, the technical details are skipped for the sake of brevity. This finishes the proof of Lemma 5.3. □

Now we perform the refined error estimate. Taking a discrete inner product with (4.2), (4.3) by $2\tilde{n}^{m+1}$, $2\tilde{p}^{m+1}$, respectively, leads to

$$\begin{aligned}
&\frac{1}{\Delta t}\Big(\|\tilde{n}^{m+1}\|_2^2-\|\tilde{n}^m\|_2^2+\|\tilde{n}^{m+1}-\tilde{n}^m\|_2^2+\|\tilde{p}^{m+1}\|_2^2-\|\tilde{p}^m\|_2^2+\|\tilde{p}^{m+1}-\tilde{p}^m\|_2^2\Big)\\
&\quad+2\Big(\big\langle\mathcal{A}(n^m)\nabla_h\tilde{\mu}_n^{m+1},\nabla_h\tilde{n}^{m+1}\big\rangle+D\big\langle\mathcal{A}(p^m)\nabla_h\tilde{\mu}_p^{m+1},\nabla_h\tilde{p}^{m+1}\big\rangle\Big)\\
=&2\big(\langle\tau_n^{m+1},\tilde{n}^{m+1}\rangle+\langle\tau_p^{m+1},\tilde{p}^{m+1}\rangle\big)\\
&\quad-2\Big(\big\langle\mathcal{A}(\tilde{n}^m)\nabla_h\mathcal{V}_n^{m+1},\nabla_h\tilde{n}^{m+1}\big\rangle+D\big\langle\mathcal{A}(\tilde{p}^m)\nabla_h\mathcal{V}_p^{m+1},\nabla_h\tilde{p}^{m+1}\big\rangle\Big).
\end{aligned}\tag{5.9}$$

The local truncation error terms could be bounded with an application of Cauchy inequality

$$\begin{aligned}
2\big\langle\tau_n^{m+1},\tilde{n}^{m+1}\big\rangle\le\big\|\tau_n^{m+1}\big\|_2^2+\big\|\tilde{n}^{m+1}\big\|_2^2,\\
2\big\langle\tau_p^{m+1},\tilde{p}^{m+1}\big\rangle\le\big\|\tau_p^{m+1}\big\|_2^2+\big\|\tilde{p}^{m+1}\big\|_2^2.
\end{aligned}\tag{5.10}$$

For the nonlinear diffusion error inner product, we begin with the following expansion:

$$\begin{aligned}
&\big\langle\mathcal{A}(n^m)\nabla_h\tilde{\mu}_n^{m+1},\nabla_h\tilde{n}^{m+1}\big\rangle\\
=&\big\langle\mathcal{A}(n^m)\nabla_h(\ln\check{\mathrm{N}}^{m+1}-\ln n^{m+1}),\nabla_h\tilde{n}^{m+1}\big\rangle+\big\langle\mathcal{A}(n^m)\nabla_h\tilde{\phi}^{m+1},\nabla_h\tilde{n}^{m+1}\big\rangle\\
&+\Big\langle\mathcal{A}(n^m)\nabla_h\big(g_{11}^c\tilde{n}^{m+1}+g_{12}^c\tilde{p}^{m+1}-g_{11}^e\tilde{n}^m-g_{12}^c\tilde{p}^m\big),\nabla_h\tilde{n}^{m+1}\Big\rangle\\
&-\sigma^n\big\langle\mathcal{A}(n^m)\nabla_h\Delta_h\tilde{n}^{m+1},\nabla_h\tilde{n}^{m+1}\big\rangle.
\end{aligned}\tag{5.11}$$

The lower bound for the second part is straightforward

$$\begin{aligned}
&\big\langle\mathcal{A}(n^m)\nabla_h\tilde{\phi}^{m+1},\nabla_h\tilde{n}^{m+1}\big\rangle\\
\ge&-\tilde{C}_3\|\nabla_h\tilde{\phi}^{m+1}\|_2\cdot\|\nabla_h\tilde{n}^{m+1}\|_2\\
\ge&-\tilde{C}_3\tilde{C}_4\|\tilde{n}^{m+1}-\tilde{p}^{m+1}\|_2\cdot\|\nabla_h\tilde{n}^{m+1}\|_2\\
\ge&-\big(\tilde{C}_3\tilde{C}_4\big)^2\big(\gamma_n^{(0)}\big)^{-1}\|\tilde{n}^{m+1}-\tilde{p}^{m+1}\|_2^2-\frac{1}{4}\gamma_n^{(0)}\|\nabla_h\tilde{n}^{m+1}\|_2.
\end{aligned}\tag{5.12}$$

The Cauchy inequality could be applied to bound the third part

$$\begin{aligned}
&\Big\langle\mathcal{A}(n^m)\nabla_h\big(g_{11}^c\tilde{n}^{m+1}+g_{12}^c\tilde{p}^{m+1}-g_{11}^e\tilde{n}^m-g_{12}^c\tilde{p}^m\big),\nabla_h\tilde{n}^{m+1}\Big\rangle\\
\ge&-\|n^m\|_\infty\cdot\big\|\nabla_h(g_{11}^c\tilde{n}^{m+1}+g_{12}^c\tilde{p}^{m+1}-g_{11}^e\tilde{n}^m-g_{12}^c\tilde{p}^m)\big\|_2\cdot\big\|\nabla_h\tilde{n}^{m+1}\big\|_2\\
\ge&-Q_n\Big(\big\|\nabla_h\tilde{n}^{m+1}\big\|_2^2+\big\|\nabla_h\tilde{p}^{m+1}\big\|_2^2+\big\|\nabla_h\tilde{n}^m\big\|_2^2+\big\|\nabla_h\tilde{p}^m\big\|_2^2\Big)
\end{aligned}\tag{5.13}$$

with

$$Q_n=\frac{1}{2}\tilde{C}_3\big(2|g_{11}^c|+|g_{12}^c|+|g_{11}^e|+|g_{12}^e|\big),$$

in which the a priori $\|\cdot\|_\infty$ estimate (4.13) has been applied. A substitution of (5.12) and (5.13), into (5.11), combined with the preliminary estimates (5.1), (5.4) (given by Lemmas 5.1, 5.3), leads to

$$
\begin{aligned}
&\left\langle \mathcal{A}(n^m)\nabla_h \tilde{\mu}_n^{m+1}, \nabla_h \tilde{n}^{m+1}\right\rangle \\
\geq &\left(\frac{3}{4}\gamma_n^{(0)} - M_n^{(2)}\right)\left\|\nabla_h \tilde{n}^{m+1}\right\|_2^2 - M_n^{(0)}\|\tilde{n}^{m+1}\|_2^2 \\
&-2\big(\tilde{C}_3\tilde{C}_4\big)^2\big(\gamma_n^{(0)}\big)^{-1}\big(\|\tilde{n}^{m+1}\|_2^2+\|\tilde{p}^{m+1}\|_2^2\big) - M_n^{(1)}h^8 + \gamma_n^{(1)}\left\|\Delta_h \tilde{n}^{m+1}\right\|_2^2 \\
&-Q_n\Big(\left\|\nabla_h \tilde{n}^{m+1}\right\|_2^2 + \left\|\nabla_h \tilde{p}^{m+1}\right\|_2^2 + \left\|\nabla_h \tilde{n}^{m}\right\|_2^2 + \left\|\nabla_h \tilde{p}^{m}\right\|_2^2\Big). \qquad (5.14)
\end{aligned}
$$

A similar lower bound could be derived for the other nonlinear error inner product on the left hand side; the details are skipped for the sake of brevity

$$
\begin{aligned}
&D\left\langle \mathcal{A}(p^m)\nabla_h \tilde{\mu}_p^{m+1}, \nabla_h \tilde{p}^{m+1}\right\rangle \\
\geq &\left(\frac{3}{4}\gamma_p^{(0)} - M_p^{(2)}\right)\left\|\nabla_h \tilde{p}^{m+1}\right\|_2^2 - M_p^{(0)}\|\tilde{p}^{m+1}\|_2^2 \\
&-2\big(D\tilde{C}_3\tilde{C}_4\big)^2\big(\gamma_p^{(0)}\big)^{-1}\Big(\|\tilde{n}^{m+1}\|_2^2+\|\tilde{p}^{m+1}\|_2^2\Big) - M_p^{(1)}h^8 + \gamma_p^{(1)}\left\|\Delta_h \tilde{n}^{m+1}\right\|_2^2 \\
&-Q_p\Big(\left\|\nabla_h \tilde{n}^{m+1}\right\|_2^2 + \left\|\nabla_h \tilde{p}^{m+1}\right\|_2^2 + \left\|\nabla_h \tilde{n}^{m}\right\|_2^2 + \left\|\nabla_h \tilde{p}^{m}\right\|_2^2\Big) \qquad (5.15)
\end{aligned}
$$

with

$$
Q_p = \frac{1}{2}D\tilde{C}_3\big(2|g_{22}^c| + |g_{21}^c| + |g_{22}^e| + |g_{21}^e|\big).
$$

The last two nonlinear error inner product terms on the right-hand side could be bounded by a direct application of Cauchy inequality

$$
\begin{aligned}
&-2\left\langle \mathcal{A}(\tilde{n}^m)\nabla_h \mathcal{V}_n^{m+1}, \nabla_h \tilde{n}^{m+1}\right\rangle \\
&\leq 2\left\|\nabla_h \mathcal{V}_n^{m+1}\right\|_\infty \cdot \left\|\mathcal{A}(\tilde{n}^m)\right\|_2 \cdot \left\|\nabla_h \tilde{n}^{m+1}\right\|_2 \\
&\leq 2C^\star \left\|\tilde{n}^m\right\|_2 \cdot \left\|\nabla_h \tilde{n}^{m+1}\right\|_2 \leq C^*\Big(\left\|\tilde{n}^m\right\|_2^2 + \left\|\nabla_h \tilde{n}^{m+1}\right\|_2^2\Big), \qquad (5.16) \\
&-2D\left\langle \mathcal{A}(\tilde{p}^m)\nabla_h \mathcal{V}_p^{m+1}, \nabla_h \tilde{p}^{m+1}\right\rangle \leq DC^\star\Big(\left\|\tilde{p}^m\right\|_2^2 + \left\|\nabla_h \tilde{p}^{m+1}\right\|_2^2\Big), \qquad (5.17)
\end{aligned}
$$

in which the regularity assumption (4.8) has been used. As a result, a substitution of (5.10), (5.14)-(5.15) and (5.16)-(5.17) into (5.9) yields

$$
\begin{aligned}
&\frac{1}{\Delta t}\Big(\|\tilde{n}^{m+1}\|_2^2 - \|\tilde{n}^m\|_2^2 + \|\tilde{p}^{m+1}\|_2^2 - \|\tilde{p}^m\|_2^2\Big) + \gamma_n^{(0)}\left\|\nabla_h \tilde{n}^{m+1}\right\|_2^2 \\
&\quad + \gamma_p^{(0)}\left\|\nabla_h \tilde{p}^{m+1}\right\|_2^2 + 2\gamma_n^{(1)}\left\|\Delta_h \tilde{n}^{m+1}\right\|_2^2 + 2\gamma_p^{(1)}\left\|\Delta_h \tilde{p}^{m+1}\right\|_2^2 \\
&\leq M^{(2)}\Big(\|\tilde{n}^{m+1}\|_2^2 + \|\tilde{p}^{m+1}\|_2^2\Big) + M^{(3)}\Big(\|\tilde{n}^m\|_2^2 + \|\tilde{p}^m\|_2^2\Big) + M^{(4)}h^8 \\
&\quad + M^{(5)}\Big(\left\|\nabla_h \tilde{n}^{m+1}\right\|_2^2 + \left\|\nabla_h \tilde{p}^{m+1}\right\|_2^2 + \left\|\nabla_h \tilde{n}^{m}\right\|_2^2 + \left\|\nabla_h \tilde{p}^{m}\right\|_2^2\Big) \\
&\quad + \left\|\tau_n^{m+1}\right\|_2^2 + \left\|\tau_p^{m+1}\right\|_2^2, \qquad (5.18)
\end{aligned}
$$

with the following constant representations:

$$M^{(2)}=4\big(\tilde{C}_3\tilde{C}_4\big)^2\left(\big(\gamma_n^{(0)}\big)^{-1}+D^2\big(\gamma_p^{(0)}\big)^{-1}\right)+2\big(M_n^{(0)}+M_p^{(0)}\big)+1, \tag{5.19}$$

$$M^{(3)}=2C^{\star}+2DC^{\star}, \tag{5.20}$$

$$M^{(4)}=2\big(M_n^{(1)}+M_p^{(1)}\big), \tag{5.21}$$

$$M^{(5)}=2\big(Q_n+Q_p+C^*+DC^*\big). \tag{5.22}$$

Meanwhile, for $k=m,m+1$, a careful application of Cauchy inequality indicates that

$$\begin{aligned}
M^{(5)}\big\|\nabla_h\tilde{n}^k\big\|_2^2 &\le M^{(5)}\big\|\tilde{n}^k\big\|_2\cdot\big\|\Delta_h\tilde{n}^k\big\|_2\\
&\le\frac{1}{2}\gamma_n^{(1)}\big\|\Delta_h\tilde{n}^k\big\|_2^2+\frac{1}{2}\big(\gamma_n^{(1)}\big)^{-1}(M^{(5)})^2\|\tilde{n}^k\|_2^2,\\
M^{(5)}\big\|\nabla_h\tilde{p}^k\big\|_2^2 &\le M^{(5)}\big\|\tilde{p}^k\big\|_2\cdot\big\|\Delta_h\tilde{p}^k\big\|_2\\
&\le\frac{1}{2}\gamma_p^{(1)}\big\|\Delta_h\tilde{p}^k\big\|_2^2+\frac{1}{2}\big(\gamma_p^{(1)}\big)^{-1}(M^{(5)})^2\|\tilde{p}^k\|_2^2.
\end{aligned} \tag{5.23}$$

Its substitution into (5.18) gives

$$\begin{aligned}
&\frac{1}{\Delta t}\Big(\|\tilde{n}^{m+1}\|_2^2-\|\tilde{n}^m\|_2^2+\|\tilde{p}^{m+1}\|_2^2-\|\tilde{p}^m\|_2^2\Big)+\gamma_n^{(0)}\big\|\nabla_h\tilde{n}^{m+1}\big\|_2^2\\
&\quad+\gamma_p^{(0)}\big\|\nabla_h\tilde{p}^{m+1}\big\|_2^2+\frac{3}{2}\gamma_n^{(1)}\big\|\Delta_h\tilde{n}^{m+1}\big\|_2^2+\frac{3}{2}\gamma_p^{(1)}\big\|\Delta_h\tilde{p}^{m+1}\big\|_2^2\\
&\quad-\frac{1}{2}\gamma_n^{(1)}\big\|\Delta_h\tilde{n}^m\big\|_2^2-\frac{1}{2}\gamma_p^{(1)}\big\|\Delta_h\tilde{p}^m\big\|_2^2\\
&\le M^{(2)}\Big(\|\tilde{n}^{m+1}\|_2^2+\|\tilde{p}^{m+1}\|_2^2\Big)+M^{(3)}\Big(\|\tilde{n}^m\|_2^2+\|\tilde{p}^m\|_2^2\Big)+M^{(4)}h^8\\
&\quad+M^{(6)}\Big(\|\tilde{n}^{m+1}\|_2^2+\|\tilde{p}^{m+1}\|_2^2+\|\tilde{n}^m\|_2^2+\|\tilde{p}^m\|_2^2\Big)+\big\|\tau_n^{m+1}\big\|_2^2+\big\|\tau_p^{m+1}\big\|_2^2
\end{aligned} \tag{5.24}$$

with

$$M^{(6)}=\max\left(\frac{1}{2}\big(\gamma_n^{(1)}\big)^{-1}(M^{(5)})^2,\frac{1}{2}\big(\gamma_p^{(1)}\big)^{-1}(M^{(5)})^2\right).$$

An application of discrete Gronwall inequality results in the desired higher order convergence estimate

$$\|\tilde{n}^{m+1}\|_2+\|\tilde{p}^{m+1}\|_2+\left(\Delta t\sum_{k=1}^{m+1}\Big(\big\|\Delta_h\tilde{n}^k\big\|_2^2+\big\|\Delta_h\tilde{p}^k\big\|_2^2\Big)\right)^{\frac{1}{2}}\le C\big(\Delta t^2+h^2\big), \tag{5.25}$$

in which the higher order truncation error accuracy, $\|\tau_n^{m+1}\|_2$, $\|\tau_p^{m+1}\|_2\le C(\Delta t^2+h^2)$, has been recalled. This completes the refined error estimate.

Recovery of the a priori assumption (4.9)

As a result of the higher order error estimate (5.25), we notice that the a priori assumption in (4.9) is satisfied at the next time step t^{m+1}

$$\|\tilde{n}^{m+1}\|_2+\|\tilde{p}^{m+1}\|_2\le C\big(\Delta t^2+h^2\big)\le \Delta t^{\frac{15}{8}}+h^{\frac{15}{8}}, \tag{5.26}$$

$$\big\|\Delta_h\tilde{n}^{m+1}\big\|_2+\big\|\Delta_h\tilde{p}^{m+1}\big\|_2\le \frac{C\big(\Delta t^2+h^2\big)}{\Delta t^{\frac{1}{2}}}\le C\Big(\Delta t^{\frac{3}{2}}+h^{\frac{3}{2}}\Big)\le \Delta t^{\frac{11}{8}}+h^{\frac{11}{8}}, \tag{5.27}$$

under the linear refinement requirement, $C_1h\le\Delta t\le C_2h$, provided that Δt and h are sufficiently small. Therefore, an induction analysis could be applied. This completes the higher order convergence analysis.

As a result, the convergence estimate (2.24) for the variable (n,p) is a direct consequence of (5.25), combined with the definition (3.1) of the constructed approximate solution $(\hat{\mathsf{N}},\hat{\mathsf{P}})$, as well as the projection estimate (2.20).

In terms of the convergence estimate for the electric potential variable ϕ, the definition for $\tilde{\phi}^k$ in (4.1) implies that

$$\big\|\tilde{\phi}^m\big\|_{H_h^2}\le C\big\|\Delta_h\tilde{\phi}^m\big\|_2\le \frac{C}{\varepsilon}\|\tilde{n}^m-\tilde{p}^m\|_2\le C\big(\Delta t^2+h^2\big). \tag{5.28}$$

As a consequence, we arrive at

$$\big\|\tilde{\phi}^m-e_\phi^m\big\|_{H_h^2}\le C\big\|\Delta_h(\tilde{\phi}^m-e_\phi^m)\big\|_2\le C\big(\Delta t+h^2\big), \tag{5.29}$$

since

$$(-\Delta_h)\big(\tilde{\phi}^m-e_\phi^m\big)=\Delta t\mathcal{P}_N(\mathsf{P}_{\Delta t,1}-\mathsf{N}_{\Delta t,1})+\tau_\phi^m. \tag{5.30}$$

In fact, the discrete elliptic regularity has been applied in (5.28), (5.29), and the truncation error for ϕ is defined as $\tau_\phi^m=(-\Delta_h)\Phi_N-(\hat{\mathsf{P}}^m-\hat{\mathsf{N}}^m)$. Therefore, we obtain

$$\big\|e_\phi^m\big\|_{H_h^2}\le\big\|\tilde{\phi}^m\big\|_{H_h^2}+\big\|\tilde{\phi}^m-e_\phi^m\big\|_{H_h^2}\le C\big(\Delta t^2+h^2\big)+C\big(\Delta t+h^2\big)\le C\big(\Delta t+h^2\big). \tag{5.31}$$

This finishes the proof of Theorem 2.3.

Remark 5.1. For the classical PNP system studied in [37], the free-energy functional of the system is convex with respect to concentrations. Meanwhile, the free-energy functional (1.4) for the PNPCH system is non-convex due to the cross interactions described by the matrix G, which could not be diagonally dominant. With regularization from high-order Cahn-Hilliard terms, some tricky difference has appeared in the convergence analysis reported in this work. The complicated nonlinear stability convergence analysis presented in [37] can be partially circumvented by taking advantage of the high-order derivative terms, while extra attention should be paid to the treatment of cross interaction terms.

6 Numerical results

To find the numerical solution to the PNPCH system, we develop a Newton's iteration method to solve the fully nonlinear scheme (2.7)-(2.10) at each time step. Given the numerical solution n^m, p^m, and ϕ^m, we initialize the Newton's iterations with $n^{m+1,0}=n^m$, $p^{m+1,0}=p^m$, and $\phi^{m+1,0}=\phi^m$. Based on the l-th iteration solution, we then obtain the $(l+1)$-th iteration by solving a linearized system

$$
\begin{aligned}
&\frac{n^{m+1,l+1}-n^m}{\Delta t}=\nabla_h\cdot\left(\check{\mathcal{M}}_n^m\nabla_h\mu_n^{m+1,l+1}\right), &(6.1)\\
&\mu_n^{m+1,l+1}=\ln n^{m+1,l}+\frac{n^{m+1,l+1}}{n^{m+1,l}}-1-\phi^{m+1,l+1}-\sigma^n\Delta_h n^{m+1,l+1}\\
&\qquad\qquad +g_{11}^c n^{m+1,l+1}+g_{12}^c p^{m+1,l+1}-g_{11}^e n^m-g_{12}^e p^m, &(6.2)\\
&\frac{p^{m+1,l+1}-p^m}{\Delta t}=\nabla_h\cdot\left(\check{\mathcal{M}}_p^m\nabla_h\mu_p^{m+1,l+1}\right), &(6.3)\\
&\mu_p^{m+1,l+1}=\ln p^{m+1,l}+\frac{p^{m+1,l+1}}{p^{m+1,l}}-1+\phi^{m+1,l+1}-\sigma^p\Delta_h p^{m+1,l+1}\\
&\qquad\qquad +g_{21}^c n^{m+1,l+1}+g_{22}^c p^{m+1,l+1}-g_{21}^e n^m-g_{22}^e p^m, &(6.4)\\
&-\nabla_h\cdot(\nabla_h\phi^{m+1,l+1})=p^{m+1,l+1}-n^{m+1,l+1}+\rho_h^f, &(6.5)
\end{aligned}
$$

where the mobility functions are given in (2.12). Discrete periodic boundary conditions are imposed for the difference equations. This is a linear system involving $n^{m+1,l+1}$, $\mu_n^{m+1,l+1}$, $p^{m+1,l+1}$, $\mu_p^{m+1,l+1}$, and $\phi^{m+1,l+1}$. For simplicity, we present the linear system in a two dimensional setting. We denote by

$$
\boldsymbol{n}^{m+1,l+1}:=\left(n_{11}^{m+1,l+1},n_{12}^{m+1,l+1},\cdots,n_{1N}^{m+1,l+1},n_{21}^{m+1,l+1},\cdots,n_{2N}^{m+1,l+1},\cdots,n_{NN}^{m+1,l+1}\right)^T
$$

the column vector consisting of the unknowns involving $n^{m+1,l+1}$. The vectors $\boldsymbol{\mu_n}^{m+1,l+1}$, $\boldsymbol{p}^{m+1,l+1}$, $\boldsymbol{\mu_p}^{m+1,l+1}$, and $\boldsymbol{\Phi}^{m+1,l+1}$ are defined analogously. In addition, we denote by the matrices $\mathcal{A}_{\mathcal{M}_n}$ and $\mathcal{A}_{\mathcal{M}_p}$ corresponding to the discrete operators $\nabla_h\cdot\check{\mathcal{M}}_n^m\nabla_h$ and $\nabla_h\cdot\check{\mathcal{M}}_p^m\nabla_h$, respectively. Also, we denote by the matrix $\mathcal{A}_{\Delta_h}$ corresponding to the discretization of the discrete Laplacian Δ_h. With such notations, the above linear system can be rewritten in a matrix form

$$
K\begin{pmatrix}\boldsymbol{n}^{m+1,l+1}\\ \boldsymbol{\mu_n}^{m+1,l+1}\\ \boldsymbol{p}^{m+1,l+1}\\ \boldsymbol{\mu_p}^{m+1,l+1}\\ \boldsymbol{\Phi}^{m+1,l+1}\end{pmatrix}=\begin{pmatrix}\boldsymbol{n}^m\\ \ln\boldsymbol{n}^{m+1,l}-1-g_{11}^e\boldsymbol{n}^m-g_{12}^e\boldsymbol{p}^m\\ \boldsymbol{p}^m\\ \ln\boldsymbol{p}^{m+1,l}-1-g_{21}^e\boldsymbol{n}^m-g_{22}^e\boldsymbol{p}^m\\ \boldsymbol{\rho}_h^f\end{pmatrix},
$$

where

$$K=\begin{pmatrix} I_{N^2} & -\Delta t\mathcal{A}_{\mathcal{M}_n} & 0 & 0 & 0 \\ \sigma^n\mathcal{A}_{\Delta_h}-g^c_{11}I_{N^2}-\mathcal{D}_n & I_{N^2} & -g^c_{12}I_{N^2} & 0 & I_{N^2} \\ 0 & 0 & I_{N^2} & -\Delta t\mathcal{A}_{\mathcal{M}_p} & 0 \\ -g^c_{21}I_{N^2} & 0 & \sigma^p\mathcal{A}_{\Delta_h}-g^c_{22}I_{N^2}-\mathcal{D}_p & I_{N^2} & -I_{N^2} \\ I_{N^2} & 0 & -I_{N^2} & 0 & -\mathcal{A}_{\Delta_h} \end{pmatrix},$$

and $\mathcal{D}_n=\text{diag}\{1/\boldsymbol{n}^{m+1,l}\}$ and $\mathcal{D}_p=\text{diag}\{1/\boldsymbol{p}^{m+1,l}\}$ are diagonal matrices with diagonal elements being the column vectors $1/\boldsymbol{n}^{m+1,l}$ and $1/\boldsymbol{p}^{m+1,l}$, respectively. The Newton's iterations stop when the change between two consecutive iterations becomes smaller than a prescribed stopping criterion.

In our numerical tests, we perform a series of numerical simulations to verify the accuracy of the proposed scheme and confirm its performance in preserving the desired properties, including positivity, mass conservation, and energy dissipation, at the discrete level. For simplicity, we consider the dynamics of the ionic concentrations and electric potential of a charge system consisting of symmetric binary electrolytes with $D=1$.

6.1 Accuracy test

We test numerical accuracy of the proposed scheme in two dimensions. We choose a computational domain $\Omega=[-4,4]^2$, and take the steric interaction coefficient matrix $G=\left(\begin{smallmatrix}3&1\\1&3\end{smallmatrix}\right)$ and gradient energy coefficients $\sigma^n=\sigma^p=0.01$. We consider the PNPCH equations with periodic boundary conditions

$$\partial_t n=\nabla\cdot\big(n\nabla(-\phi+\ln n+g_{11}n+g_{12}p-\sigma^n\Delta n)\big)+f_n, \tag{6.6}$$

$$\partial_t p=\nabla\cdot\big(Dp\nabla(\phi+\ln p+g_{21}n+g_{22}p-\sigma^p\Delta p)\big)+f_p, \tag{6.7}$$

$$-\Delta\phi=p-n+\rho^f, \tag{6.8}$$

where the sources terms f_n, f_p, ρ^f, and the initial conditions are determined by the constructed exact solution

$$\begin{cases} n=0.2e^{-t}\cos\left(\dfrac{\pi x}{4}\right)\sin\left(\dfrac{\pi y}{4}\right)+1, \\ p=0.2e^{-t}\cos\left(\dfrac{\pi x}{4}\right)\sin\left(\dfrac{\pi y}{4}\right)+1, \\ \phi=e^{-t}\cos(\pi x)\sin(\pi y). \end{cases}$$

We carry out a series of simulations on various mesh resolutions with $\Delta t=h^2$ and compute the error with the exact solution. From Table 1, one can observe that the numerical solutions of the ion concentrations and electric potential both converge to the exact solution with a convergence order about 2, showing that the proposed numerical scheme has the anticipated convergence accuracy.

Table 1: The ℓ^∞ error and convergence order for numerical solutions of p,n, and ϕ at $T=0.16$ with a mesh ratio $\Delta t = h^2$.

N	ℓ^∞ error in n	Order	ℓ^∞ error in p	Order	ℓ^∞ error in ϕ	Order
60	2.70e-3	-	2.70e-3	-	1.54e-2	-
80	1.50e-3	2.04	1.50e-3	2.04	8.10e-3	2.23
100	9.81e-4	1.91	9.81e-4	1.91	5.10e-3	2.07
120	6.85e-4	1.97	6.85e-4	1.97	3.50e-3	2.07

6.2 Properties test and steric effect

In this case, we assess the performance of our numerical scheme in maintaining the physical properties and capturing ionic steric effects. We consider a computational domain $\Omega = [-1,1]^2$ with periodic boundary conditions and the charge distribution function

$$\begin{aligned}\rho^f(x,y) = & e^{-100[(x+0.5)^2+(y+0.5)^2]} - e^{-100[(x+0.5)^2+(y-0.5)^2]} \\ & - e^{-100[(x-0.5)^2+(y+0.5)^2]} + e^{-100[(x-0.5)^2+(y-0.5)^2]}. \end{aligned} \tag{6.9}$$

We take the steric interaction coefficient matrix $G = \begin{pmatrix} 1 & 15 \\ 15 & 1 \end{pmatrix}$, the gradient energy coefficients $\sigma^n = \sigma^p = 0.0005$. In our numerical simulations, we take the grid number $N = 100$ and a mesh ratio $\Delta t = h/2$.

Fig. 1 (left) displays the snapshots of concentrations and ϕ at different times. Starting from a uniform initial distribution $n(0,x,y) = p(0,x,y) = 0.1$, the ions move along the gradient of the electrostatic potential generated by the fixed charges. At $T = 0.5$, one can see that ions are densely accumulated in the vicinity of oppositely charged fixed charges, with the emergence of oscillations along the radial direction. Such an overscreening structure has

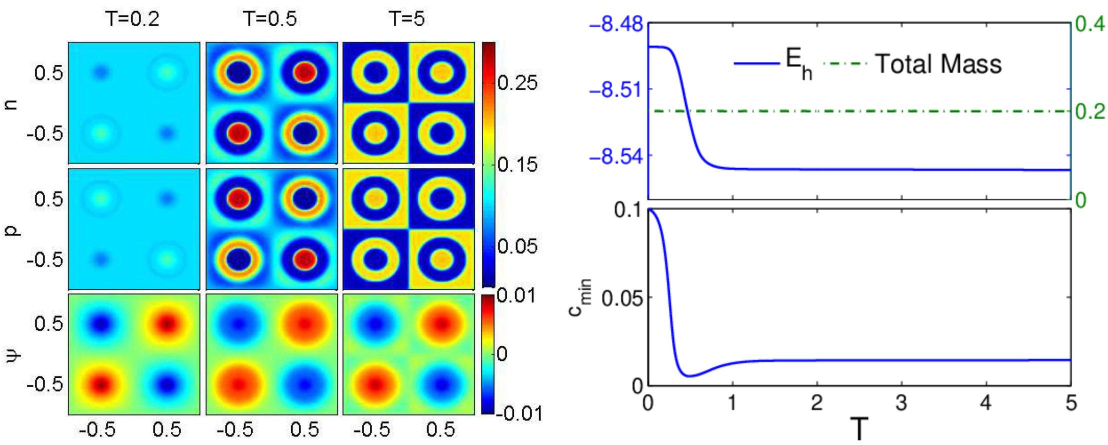

Figure 1: Left: Snapshots on the dynamics of p,n and ϕ starting from a uniform initial ionic distribution $n(0,x,y) = p(0,x,y) = 0.1$. Right: The evolution of discrete energy E_h, total mass, and minimum concentration value of both cations and anions.

been observed in the work [3]. As time evolves, the peaks of ion concentrations decrease when the energy gradient terms that penalize large concentration gradients gradually come into play. Meanwhile, the oscillation pattern emerges not only in the electric double layer but also in the bulk. Overall, one can find that the electrostatic interactions dominate the ion dynamics in the early stage, and the effect of phase separation comes into effect later in the development of rich self-assembly nanostructuring patterns.

As revealed in Fig. 1 (left), electrodiffusion and phase separation come into play in different stages of the pattern formation, displaying charge dynamics of multiple time scales. This is further confirmed by the history of the free energy of the system, as shown in the Fig. 1 (right). One can see that the free energy decays monotonically, indicating that our numerical scheme is energy stable. Also, the free energy has a plateau in the first stage and then relaxes eventually to an equilibrium that corresponds to the emergence of self-assembly nanostructuring patterns in the bulk. Such a multi-phase free-energy dissipation is reminiscent of the metastability phenomena [23]. Multi-phase free-energy dissipation with metastability often requires long-time simulations, which stress the need for robust, energy stable numerical schemes that allow large time stepping. Our numerical tests demonstrate that the proposed numerical scheme is able to effectively capture such multi-phase dynamics. In addition, one can see from the upper plot of Fig. 1 (right) that the total mass of ions, shown in the dashed line, remains constant for all the time. The lower plot depicts the evolution of $c_{\min}$, the minimum value of n and p on the computational mesh, indicating that our numerical scheme can preserve positivity at discrete level.

To understand ionic steric effects, we perform simulations with the classical PNP model that is obtained by simply setting the matrix $G=0$ and the gradient energy coefficients $\sigma^n=\sigma^p=0$. From Fig. 2 (left), one can see totally different dynamics. Both the ionic concentrations and electrostatic potential are monotonically decreasing along the radial direction without forming nanostructuring patterns. Furthermore, the Fig. 2 (right) demonstrates that the energy relaxes quickly and monotonically to the equilibrium. In contrast to Fig. 1, one can see that the ionic steric effects, modeled by the cross interactions and energy gradient terms, are no longer negligible in the description of charge dynamics of concentrated electrolytes [5,21,23].

To further investigate nanostructuring patterns, we carry out simulations with the same parameters as in Fig. 1, while starting from a random initial ionic distribution that is rescaled to have the same total mass. From Fig. 3, one can see a comparison with Fig. 1 that, under random perturbations, the instability drives ions to develop labyrinthine patterns extending into the bulk [23]. The non-convexity of the free-energy functional, due to the cross interaction terms, is responsible for the different results displayed in Figs. 1 and 3, which share the same parameters but different initial conditions. It is of interest to see that the free energy dissipation exhibits two clear stages. The first stage corresponds to the quick smoothing of random initial ionic distributions. After passing a plateau, the self-assembly labyrinthine pattern emerges in the second stage and the system reaches an equilibrium eventually.

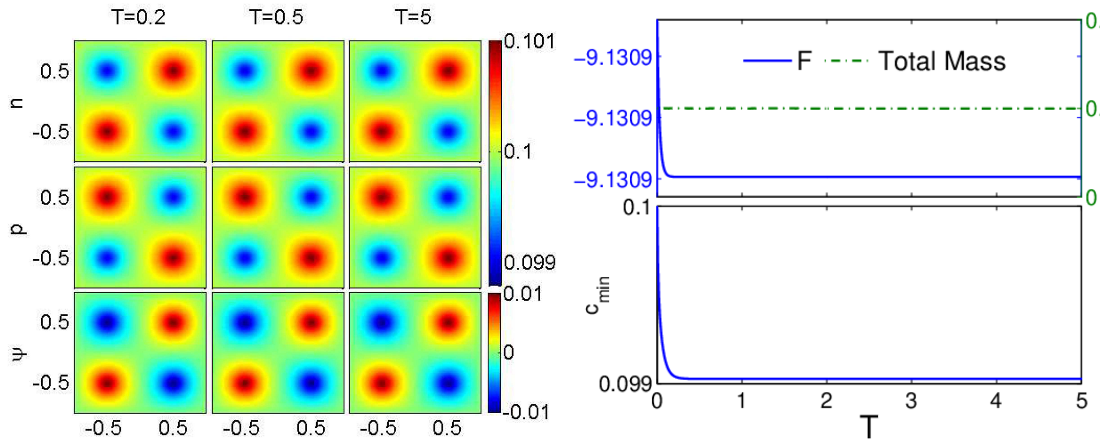

Figure 2: Left: Snapshots on the dynamics of p,n and ϕ calculated by the classical PNP model starting from a uniform initial ionic distribution $n(0,x,y)=p(0,x,y)=0.1$. Right: The evolution of discrete energy E_h, total mass, and minimum concentration value of both cations and anions.

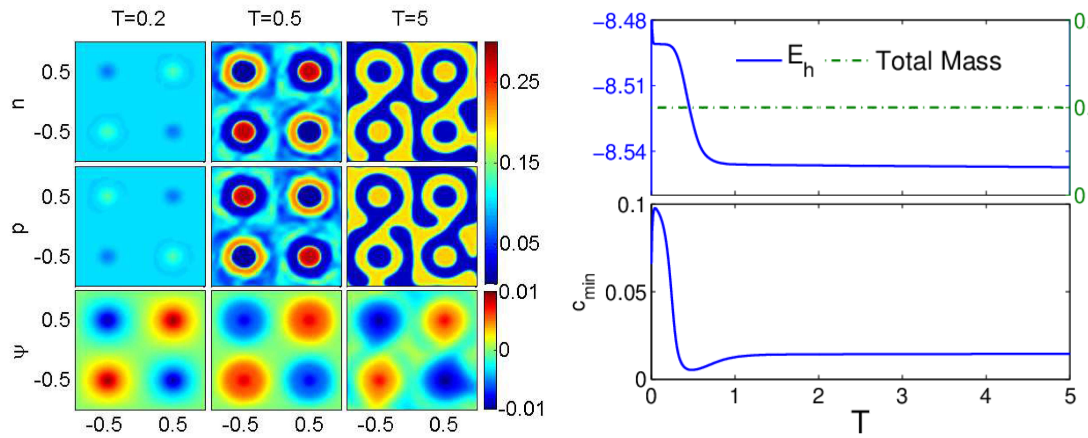

Figure 3: Left: Snapshots on the dynamics of p,n and ϕ starting from a random initial ionic distribution with a given total mass. Right: The evolution of discrete energy E_h, total mass, and minimum concentration value of both cations and anions.

7 Concluding remarks

An optimal rate convergence analysis and error estimate has been presented for a structure-preserving finite difference scheme for the Poisson-Nernst-Planck-Cahn-Hilliard (PNPCH) system, based on the Energetic Variational Approach (EnVarA) of the physical model. In such a numerical scheme, the mobility function has been explicitly treated to ensure the unique solvability, while both the nonlinear singular logarithmic and the surface diffusion terms have been implicitly updated. Such a treatment comes from the convex nature of the corresponding energy parts. A convex splitting numerical method has been applied to treat the steric interaction terms. The most distinguished challenge has been associated with the non-constant mobility nature of the physical system, nonlinear parabolic coefficients in the gradient flow, as well as the singularity in the logarithmic terms. To overcome this subtle difficulty, an asymptotic expansion of the numerical solution (in terms of the time step size) has been performed, so that a higher order consistency order can be obtained. Subsequently, the rough error estimate has led to an ℓ^∞ bound for ion concentrations, so that the phase separation property becomes available for the numerical solution at both the previous and next time steps. Finally, a refined error estimate has been performed, and the desired convergence estimate has been accomplished, in the $\ell^\infty(0,T;\ell^2)\cap\ell^2(0,T;H_h^2)$ norm. Numerical tests have demonstrated that our numerical scheme has expected convergence order and is capable of preserving mass conservation, positivity, and free-energy dissipation at discrete level.

Appendix A. Proof of Lemma 5.1

Looking at a single mesh cell $(i,j,k)\to(i+1,j,k)$, we make the following observation:

$$\begin{aligned}
&D_x\big(\ln\hat{\mathsf{N}}^{m+1}-\ln n^{m+1}\big)_{i+\frac12,j,k}\\
=&\frac{1}{h}\Big(\ln\hat{\mathsf{N}}^{m+1}_{i+1,j,k}-\ln\hat{\mathsf{N}}^{m+1}_{i,j,k}\Big)-\frac{1}{h}\Big(\ln n^{m+1}_{i+1,j,k}-\ln n^{m+1}_{i,j,k}\Big)\\
=&\frac{1}{\xi_{\mathsf{N}}}D_x\hat{\mathsf{N}}^{m+1}_{i+\frac12,j,k}-\frac{1}{\xi_n}D_x n^{m+1}_{i+\frac12,j,k}\\
=&\left(\frac{1}{\xi_{\mathsf{N}}}-\frac{1}{\xi_n}\right)D_x\hat{\mathsf{N}}^{m+1}_{i+\frac12,j,k}+\frac{1}{\xi_n}D_x\tilde{n}^{m+1}_{i+\frac12,j,k},
\end{aligned}\tag{A.1}$$

in which the mean value theorem has been repeatedly applied, where

$$\begin{aligned}
&\xi_{\mathsf{N}} \quad \text{is between} \quad \hat{\mathsf{N}}^{m+1}_{i+1,j,k} \quad \text{and} \quad \hat{\mathsf{N}}^{m+1}_{i,j,k},\\
&\xi_n \quad \text{is between} \quad n^{m+1}_{i+1,j,k} \quad \text{and} \quad n^{m+1}_{i,j,k}.
\end{aligned}\tag{A.2}$$

In turn, its product with $D_x\tilde{n}^{m+1}_{i+1/2,j,k}$ leads to

$$\begin{aligned}
&D_x\tilde{n}^{m+1}_{i+\frac12,j,k}\cdot D_x(\ln\hat{\mathsf{N}}^{m+1}-\ln n^{m+1})_{i+\frac12,j,k}\\
=&\left(\frac{1}{\xi_{\mathsf{N}}}-\frac{1}{\xi_n}\right)D_x\hat{\mathsf{N}}^{m+1}_{i+\frac12,j,k}\cdot D_x\tilde{n}^{m+1}_{i+\frac12,j,k}+\frac{1}{\xi_n}\Big|D_x\tilde{n}^{m+1}_{i+\frac12,j,k}\Big|^2.
\end{aligned}\tag{A.3}$$

For the second part, the rough $\|\cdot\|_\infty$ estimate (4.41) for n^{m+1} implies that $0<\xi_n\le\tilde{C}_3$, which in turn gives

$$\frac{1}{\xi_n}\ge\frac{1}{\tilde{C}_3},\quad \frac{1}{\xi_n}\Big|D_x\tilde{n}^{m+1}_{i+\frac12,j,k}\Big|^2\ge\frac{1}{\tilde{C}_3}\Big|D_x\tilde{n}^{m+1}_{i+\frac12,j,k}\Big|^2.\tag{A.4}$$

For the first term on the right-hand side of (A.3), we begin with the following identity:

$$\frac{1}{\xi_{\mathsf{N}}}=\frac{\ln\hat{\mathsf{N}}^{m+1}_{i+1,j,k}-\ln\hat{\mathsf{N}}^{m+1}_{i,j,k}}{\hat{\mathsf{N}}^{m+1}_{i+1,j,k}-\hat{\mathsf{N}}^{m+1}_{i,j,k}}=\frac{\ln\big(1+(\hat{\mathsf{N}}^{m+1}_{i+1,j,k}-\hat{\mathsf{N}}^{m+1}_{i,j,k})/\hat{\mathsf{N}}^{m+1}_{i,j,k}\big)}{\hat{\mathsf{N}}^{m+1}_{i+1,j,k}-\hat{\mathsf{N}}^{m+1}_{i,j,k}}.\tag{A.5}$$

By setting

$$t_N^{(0)}=\frac{\mathsf{N}_{i+1,j,k}^{m+1}-\mathsf{N}_{i,j,k}^{m+1}}{\mathsf{N}_{i,j,k}^{m+1}},$$

the following Taylor expansion is available:

$$\ln\left(1+t_N^{(0)}\right)=t_N^{(0)}-\frac{1}{2}\left(t_N^{(0)}\right)^2+\frac{1}{3}\left(t_N^{(0)}\right)^3-\frac{1}{4}\left(t_N^{(0)}\right)^4+\frac{1}{5(1+\eta_N)^5}\left(t_N^{(0)}\right)^5 \tag{A.6}$$

with η_N between 0 and $t_N^{(0)}$. Its substitution into (A.5) yields

$$\begin{aligned}\frac{1}{\xi_{\mathsf{N}}}=&\frac{1}{\hat{\mathsf{N}}_{i,j,k}^{m+1}}-\frac{\hat{\mathsf{N}}_{i+1,j,k}^{m+1}-\hat{\mathsf{N}}_{i,j,k}^{m+1}}{2\big(\hat{\mathsf{N}}_{i,j,k}^{m+1}\big)^2}+\frac{\big(\hat{\mathsf{N}}_{i+1,j,k}^{m+1}-\hat{\mathsf{N}}_{i,j,k}^{m+1}\big)^2}{3\big(\hat{\mathsf{N}}_{i,j,k}^{m+1}\big)^3}-\frac{\big(\hat{\mathsf{N}}_{i+1,j,k}^{m+1}-\hat{\mathsf{N}}_{i,j,k}^{m+1}\big)^3}{4\big(\hat{\mathsf{N}}_{i,j,k}^{m+1}\big)^4}\\&+\frac{1}{5(1+\eta_N)^5}\frac{\big(\hat{\mathsf{N}}_{i+1,j,k}^{m+1}-\hat{\mathsf{N}}_{i,j,k}^{m+1}\big)^4}{\big(\hat{\mathsf{N}}_{i,j,k}^{m+1}\big)^5}.\end{aligned}\tag{A.7}$$

A similar equality could be derived for $1/\xi_n$

$$\begin{aligned}\frac{1}{\xi_n}=&\frac{1}{n_{i,j,k}^{m+1}}-\frac{n_{i+1,j,k}^{m+1}-n_{i,j,k}^{m+1}}{2\big(n_{i,j,k}^{m+1}\big)^2}+\frac{\big(n_{i+1,j,k}^{m+1}-n_{i,j,k}^{m+1}\big)^2}{3\big(n_{i,j,k}^{m+1}\big)^3}-\frac{\big(n_{i+1,j,k}^{m+1}-n_{i,j,k}^{m+1}\big)^3}{4\big(n_{i,j,k}^{m+1}\big)^4}\\&+\frac{1}{5(1+\eta_n)^5}\frac{\big(n_{i+1,j,k}^{m+1}-n_{i,j,k}^{m+1}\big)^4}{\big(n_{i,j,k}^{m+1}\big)^5}\end{aligned}\tag{A.8}$$

with η_n between 0 and

$$t_n^{(0)}=\frac{n_{i+1,j,k}^{m+1}-n_{i,j,k}^{m+1}}{n_{i,j,k}^{m+1}}.$$

In addition, the following estimates are derived:

$$\left|\frac{1}{\hat{\mathsf{N}}_{i,j,k}^{m+1}}-\frac{1}{n_{i,j,k}^{m+1}}\right|=\left|\frac{\tilde{n}_{i,j,k}^{m+1}}{\hat{\mathsf{N}}_{i,j,k}^{m+1}n_{i,j,k}^{m+1}}\right|\le\frac{2}{(\epsilon_0^\star)^2}\left|\tilde{n}_{i,j,k}^{m+1}\right|, \tag{A.9}$$

and

$$\begin{aligned}&\left|\frac{\hat{\mathsf{N}}_{i+1,j,k}^{m+1}-\hat{\mathsf{N}}_{i,j,k}^{m+1}}{\big(\hat{\mathsf{N}}_{i,j,k}^{m+1}\big)^2}-\frac{n_{i+1,j,k}^{m+1}-n_{i,j,k}^{m+1}}{\big(n_{i,j,k}^{m+1}\big)^2}\right|\\\le&\left|\frac{\tilde{n}_{i+1,j,k}^{m+1}-\tilde{n}_{i,j,k}^{m+1}}{\big(n_{i,j,k}^{m+1}\big)^2}\right|+\left|\frac{\big(\hat{\mathsf{N}}_{i+1,j,k}^{m+1}-\hat{\mathsf{N}}_{i,j,k}^{m+1}\big)\big(n_{i+1,j,k}^{m+1}-\hat{\mathsf{N}}_{i,j,k}^{m+1}\big)\tilde{n}_{i,j,k}^{m+1}}{\big(\hat{\mathsf{N}}_{i,j,k}^{m+1}\big)^2\big(n_{i,j,k}^{m+1}\big)^2}\right|\end{aligned}$$

$$\le \frac{4}{(\epsilon_0^\star)^2}\Big(\big|\tilde{n}_{i,j,k}^{m+1}\big|+\big|\tilde{n}_{i+1,j,k}^{m+1}\big|\Big)+\frac{2C^\star(C^\star+\tilde{C}_3)}{\frac{1}{4}(\epsilon_0^\star)^4}\big|\tilde{n}_{i,j,k}^{m+1}\big|$$
$$\le Q^{(2)}\Big(\big|\tilde{n}_{i,j,k}^{m+1}\big|+\big|\tilde{n}_{i+1,j,k}^{m+1}\big|\Big), \tag{A.10}$$

where

$$Q^{(2)}:=\frac{4}{(\epsilon_0^\star)^2}+\frac{8C^\star(C^\star+\tilde{C}_3)}{(\epsilon_0^\star)^4},$$

and the rough $\|\cdot\|_\infty$ estimate (4.41), the regularity assumption (3.19), and the separation property (3.18) have been extensively applied. The two other difference terms could be similarly analyzed

$$\left|\frac{\big(\hat{\mathsf{N}}_{i+1,j,k}^{m+1}-\hat{\mathsf{N}}_{i,j,k}^{m+1}\big)^2}{\big(\hat{\mathsf{N}}_{i,j,k}^{m+1}\big)^3}-\frac{\big(n_{i+1,j,k}^{m+1}-n_{i,j,k}^{m+1}\big)^2}{\big(n_{i,j,k}^{m+1}\big)^3}\right|\le Q^{(3)}\Big(\big|\tilde{n}_{i,j,k}^{m+1}\big|+\big|\tilde{n}_{i+1,j,k}^{m+1}\big|\Big), \tag{A.11}$$
$$\left|\frac{\big(\hat{\mathsf{N}}_{i+1,j,k}^{m+1}-\hat{\mathsf{N}}_{i,j,k}^{m+1}\big)^3}{\big(\hat{\mathsf{N}}_{i,j,k}^{m+1}\big)^4}-\frac{\big(n_{i+1,j,k}^{m+1}-n_{i,j,k}^{m+1}\big)^3}{\big(n_{i,j,k}^{m+1}\big)^4}\right|\le Q^{(4)}\Big(\big|\tilde{n}_{i,j,k}^{m+1}\big|+\big|\tilde{n}_{i+1,j,k}^{m+1}\big|\Big),$$

where $Q^{(3)}$, $Q^{(4)}$ only depend on $\epsilon_0^\star$, $C^\star$ and $\tilde{C}_3$. For the remainder terms, we observe that

$$\Big|\hat{\mathsf{N}}_{i+1,j,k}^{m+1}-\hat{\mathsf{N}}_{i,j,k}^{m+1}\Big|=h\Big|D_x\hat{\mathsf{N}}_{i+\frac{1}{2},j,k}^{m+1}\Big|\le h\|D_x\hat{\mathsf{N}}^{m+1}\|_\infty\le C^\star h, \tag{A.12}$$
$$\big|t_N^{(0)}\big|=\left|\frac{\hat{\mathsf{N}}_{i+1,j,k}^{m+1}-\hat{\mathsf{N}}_{i,j,k}^{m+1}}{\hat{\mathsf{N}}_{i,j,k}^{m+1}}\right|\le C^\star(\epsilon_0^\star)^{-1}h\le Q^{(5)}h\le\frac{1}{2}, \tag{A.13}$$

where $Q^{(5)}=C^\star(\epsilon_0^\star)^{-1}$ and where we have used $\epsilon_0^\star\le\mathsf{N}_{i,j,k}^{m+1}$. Furthermore $|\eta_N|\le 1/2$, so that

$$|1+\eta_N|\ge\frac{1}{2},\quad\left|\frac{1}{5(1+\eta_N)^5}\right|\le\frac{32}{5}. \tag{A.14}$$

Finally,

$$\big|(\mathcal{R}_1)_{i+\frac{1}{2},j,k}\big|=\left|\frac{1}{5(1+\eta_N)^5}\frac{\big(\hat{\mathsf{N}}_{i+1,j,k}^{m+1}-\hat{\mathsf{N}}_{i,j,k}^{m+1}\big)^4}{(\hat{\mathsf{N}}_{i,j,k}^{m+1})^5}\right|\le\frac{32}{5}\cdot\frac{(C^\star h)^4}{(\epsilon_0^\star)^5}\le Q^{(6)}h^4 \tag{A.15}$$

with

$$Q^{(6)}=\frac{32(C^\star)^4}{5(\epsilon_0^\star)^5}.$$

The other remainder term has a similar bound

$$\big|(\mathcal{R}_2)_{i+\frac{1}{2},j,k}\big|=\left|\frac{1}{5(1+\eta_n)^5}\frac{\big(n_{i+1,j,k}^{m+1}-n_{i,j,k}^{m+1}\big)^4}{\big(n_{i,j,k}^{m+1}\big)^5}\right|$$

$$\leq \frac{32}{5}\cdot\frac{\left(hD_x n^{m+1}_{i+\frac{1}{2},j,k}\right)^4}{(1/32)(\epsilon_0^\star)^5} \leq Q^{(7)}h^4\left|D_x n^{m+1}_{i+\frac{1}{2},j,k}\right|^4 \tag{A.16}$$

with

$$Q^{(7)} = \frac{1024}{5(\epsilon_0^\star)^5}.$$

Meanwhile, by the rough error estimate (4.43), the following $\|\cdot\|_2$ estimate could be derived for $\mathcal{R}_2$:

$$\|\mathcal{R}_2\|_2 \leq Q^{(7)}h^4\|\nabla_h n^{m+1}\|_8^4 \leq Q^{(8)}h^4, \quad Q^{(8)} := (\tilde{C}_3)^4 Q^{(7)}. \tag{A.17}$$

Consequently, a combination of (A.9)-(A.11), (A.15) and (A.16)-(A.17) indicates that

$$\left|\frac{1}{\xi_{\mathsf{N}}} - \frac{1}{\xi_n}\right| \leq Q^{(0)}\left(|\tilde{n}^{m+1}_{i,j,k}| + |\tilde{n}^{m+1}_{i+1,j,k}|\right) + Q^{(6)}h^4 + \left|(\mathcal{R}_2)_{i+\frac{1}{2},j,k}\right| \tag{A.18}$$

with

$$Q^{(0)} = \frac{2}{(\epsilon_0^\star)^2} + \frac{1}{2}Q^{(2)} + \frac{1}{3}Q^{(3)} + \frac{1}{4}Q^{(4)}.$$

Then we arrive at an estimate for the first part on the right-hand side of (A.3)

$$\begin{aligned}
&\left(\frac{1}{\xi_{\mathsf{N}}} - \frac{1}{\xi_n}\right) D_x \mathsf{N}^{m+1}_{i+\frac{1}{2},j,k}\cdot D_x\tilde{n}^{m+1}_{i+\frac{1}{2},j,k} \qquad (A.19)\\
\geq& -\left(Q^{(0)}\left(|\tilde{n}^{m+1}_{i,j,k}| + |\tilde{n}^{m+1}_{i+1,j,k}|\right) + Q^{(6)}h^4 + \left|(\mathcal{R}_2)_{i+\frac{1}{2},j,k}\right|\right)\cdot C^\star\cdot\left|D_x\tilde{n}^{m+1}_{i+\frac{1}{2},j,k}\right|\\
\geq& -\left(Q^{(0)}\left(|\tilde{n}^{m+1}_{i,j,k}| + |\tilde{n}^{m+1}_{i+1,j,k}|\right) + Q^{(6)}h^4 + \left|(\mathcal{R}_2)_{i+\frac{1}{2},j,k}\right|\right)^2 (C^\star)^2\tilde{C}_3 - (4\tilde{C}_3)^{-1}\left|D_x\tilde{n}^{m+1}_{i+\frac{1}{2},j,k}\right|^2.
\end{aligned}$$

Subsequently, a combination of (A.3), (A.4) and (A.19) results in

$$\begin{aligned}
&D_x\tilde{n}^{m+1}_{i+\frac{1}{2},j,k}\cdot D_x(\ln\hat{\mathsf{N}}^{m+1} - \ln n^{m+1})_{i+\frac{1}{2},j,k}\\
\geq& -\left(Q^{(0)}\left(|\tilde{n}^{m+1}_{i,j,k}| + |\tilde{n}^{m+1}_{i+1,j,k}|\right) + Q^{(6)}h^4 + \left|(\mathcal{R}_2)_{i+1/2,j,k}\right|\right)^2 (C^\star)^2\tilde{C}_3 + \frac{3}{4\tilde{C}_3}\left|D_x\tilde{n}^{m+1}_{i+\frac{1}{2},j,k}\right|^2\\
\geq& \frac{3}{4\tilde{C}_3}\left|D_x\tilde{n}^{m+1}_{i+\frac{1}{2},j,k}\right|^2 - 6\left(Q^{(0)}C^\star\right)^2\tilde{C}_3\left(|\tilde{n}^{m+1}_{i,j,k}|^2 + |\tilde{n}^{m+1}_{i+1,j,k}|^2\right) - 3(Q^\star C^\star)^2\tilde{C}_3 h^8\\
&-3(C^\star)^2\tilde{C}_3\left|(\mathcal{R}_2)_{i+\frac{1}{2},j,k}\right|^2. \qquad (A.20)
\end{aligned}$$

Notice that this inequality is valid at a point-wise level. With summation over space, and keeping in mind of the a priori $\|\cdot\|_\infty$ estimate (4.13), (4.15) for n^m, combined with the $\|\cdot\|_2$ estimate (A.17) for $\mathcal{R}_2$, we obtain

$$\begin{aligned}
&\left\langle \mathcal{A}(n^m)\nabla_h\left(\ln\hat{\mathsf{N}}^{m+1} - \ln n^{m+1}\right), \nabla_h\tilde{n}^{m+1}\right\rangle\\
\geq& \frac{\epsilon_0^\star}{2}\cdot\frac{3}{4\tilde{C}_3}\|\nabla_h\tilde{n}^{m+1}\|_2^2 - 12\left(Q^{(0)}C^\star\right)^2\tilde{C}_3^2\|\tilde{n}^{m+1}\|_2^2 - 3\left(Q^{(6)}C^\star\right)^2\tilde{C}_3^2|\Omega|h^8 - 3(C^\star)^2\tilde{C}_3^2\|\mathcal{R}_2\|_2^2\\
\geq& \frac{3\epsilon_0^\star}{8\tilde{C}_3}\|\nabla_h\tilde{n}^{m+1}\|_2^2 - 12\left(Q^{(0)}C^\star\right)^2\tilde{C}_3^2\|\tilde{n}^{m+1}\|_2^2 - 3(C^\star)^2\tilde{C}_3^2\left(\left(Q^{(6)}\right)^2|\Omega| + \left(Q^{(8)}\right)^2\right)h^8. \qquad (A.21)
\end{aligned}$$

This proves the first nonlinear estimate (5.1), by setting

$$\gamma_n^{(0)} = \frac{3\epsilon_0^\star}{8\tilde{C}_3}, \quad M_n^{(0)} = 12\big(Q^{(0)}C^\star\big)^2\tilde{C}_3^2, \quad M_n^{(1)} = 3(C^\star)^2\tilde{C}_3^2\Big(\big(Q^{(6)}\big)^2|\Omega| + \big(Q^{(8)}\big)^2\Big).$$

The second nonlinear estimate (5.2) could be derived exactly in the same manner. The details are skipped for the sake of brevity.

Acknowledgements

This work was supported by the National Science Foundation (USA) Grant NSF DMS-2012669 (C. Wang), National Natural Science Foundation of China Grant 12171319, Natural Science Foundation of Jiangsu Province Grant BK20200098, Young Elite Scientist Sponsorship Program by Jiangsu Association for Science and Technology, and Shanghai Science and Technology Commission Grant 21JC1403700 (Y. Qian and S. Zhou).

References

[1] A. Baskaran, J. Lowengrub, C. Wang, and S. Wise, *Convergence analysis of a second order convex splitting scheme for the modified phase field crystal equation*, SIAM J. Numer. Anal., 51:2851–2873, 2013.

[2] M. Bazant, M. S. Kilic, B. D. Storey, and A. Ajdari, *Towards an understanding of induced-charge electrokinetics at large applied voltages in concentrated solutions*, Adv. Colloid. Interface Sci., 152:48–88, 2009.

[3] M. Bazant, B. D. Storey, and A. A. Kornyshev, *Double layer in ionic liquids: Overscreening versus crowding*, Phys. Rev. Lett., 106:046102, 2011.

[4] M. Bazant, K. Thornton, and A. Ajdari, *Diffuse-charge dynamics in electrochemical systems*, Phys. Rev. E, 70:021506, 2004.

[5] S. Bier, N. Gavish, H. Uecker, and A. Yochelis, *From bulk self-assembly to electrical diffuse layer in a continuum approach for ionic liquids: The impact of anion and cation size asymmetry*, Phys. Rev. E, 95:060201, 2017.

[6] I. Borukhov, D. Andelman, and H. Orland, *Steric effects in electrolytes: A modified Poisson-Boltzmann equation*, Phys. Rev. Lett., 79:435–438, 1997.

[7] W. Chen, C. Wang, X. Wang, and S. Wise, *Positivity-preserving, energy stable numerical schemes for the Cahn-Hilliard equation with logarithmic potential*, J. Comput. Phys. X, 3:100031, 2019.

[8] J. Ding, C. Wang, and S. Zhou, *Optimal rate convergence analysis of a second order numerical scheme for the Poisson-Nernst-Planck system*, Numer. Math. Theory Methods Appl., 12:607–626, 2019.

[9] J. Ding, Z. Wang, and S. Zhou, *Positivity preserving finite difference methods for Poisson-Nernst-Planck equations with steric interactions: Application to slit-shaped nanopore conductance*, J. Comput. Phys., 397:108864, 2019.

[10] J. Ding, Z. Wang, and S. Zhou, *Structure-preserving and efficient numerical methods for ion transport*, J. Comput. Phys., 418:109597, 2020.

[11] L. Dong, W. Feng, C. Wang, S. Wise, and Z. Zhang, *Convergence analysis and numerical implementation of a second order numerical scheme for the three-dimensional phase field crystal equation*, Comput. Math. Appl., 75:1912–1928, 2018.

[12] L. Dong, C. Wang, S. Wise, and Z. Zhang, *A positivity-preserving, energy stable scheme for a ternary Cahn-Hilliard system with the singular interfacial parameters*, J. Comput. Phys., 442: 110451, 2021.

[13] L. Dong, C. Wang, H. Zhang, and Z. Zhang, *A positivity-preserving, energy stable and convergent numerical scheme for the Cahn-Hilliard equation with a Flory-Huggins-deGennes energy*, Commun. Math. Sci., 17:921–939, 2019.

[14] L. Dong, C. Wang, H. Zhang, and Z. Zhang, *A positivity-preserving second-order BDF scheme for the Cahn-Hilliard equation with variable interfacial parameters*, Commun. Comput. Phys., 28:967–998, 2020.

[15] C. Duan, C. Liu, C. Wang, and X. Yue, *Convergence analysis of a numerical scheme for the porous medium equation by an energetic variational approach*, Numer. Math. Theory Methods Appl., 13:1–18, 2020.

[16] W. E and J.-G. Liu, *Projection method I: Convergence and numerical boundary layers*, SIAM J. Numer. Anal., 32:1017–1057, 1995.

[17] W. E and J.-G. Liu, *Projection method III. Spatial discretization on the staggered grid*, Math. Comp., 71:27–47, 2002.

[18] B. Eisenberg, Y. Hyon, and C. Liu, *Energy variational analysis of ions in water and channels: Field theory for primitive models of complex ionic fluids*, J. Chem. Phys., 133:104104, 2010.

[19] A. Flavell, M. Machen, R. Eisenberg, J. Kabre, C. Liu, and X. Li, *A conservative finite difference scheme for Poisson-Nernst-Planck equations*, J. Comput. Electron., 13:235–249, 2014.

[20] N. Gavish, *Poisson-Nernst-Planck equations with steric effects – non-convexity and multiple stationary solutions*, Phys. D, 368:50–65, 2018.

[21] N. Gavish, D. Elad, and A. Yochelis, *From solvent-free to dilute electrolytes: Essential components for a continuum theory*, J. Phys. Chem. Lett., 9:36–42, 2018.

[22] N. Gavish, C. Liu, and B. Eisenberg, *Do bistable steric Poisson-Nernst-Planck models describe single-channel gating?*, J. Phys. Chem. B, 22(20):5183–5192, 2018.

[23] N. Gavish and A. Yochelis, *Theory of phase separation and polarization for pure ionic liquids*, J. Phys. Chem. Lett., 7:1121–1126, 2016.

[24] Z. Guan, J. Lowengrub, and C. Wang, *Convergence analysis for second order accurate schemes for the periodic nonlocal Allen-Cahn and Cahn-Hilliard equations*, Math. Methods Appl. Sci., 40: 6836–6863, 2017.

[25] Z. Guan, C. Wang, and S. Wise, *A convergent convex splitting scheme for the periodic nonlocal Cahn-Hilliard equation*, Numer. Math., 128:377–406, 2014.

[26] J. Guo, C. Wang, S. Wise, and X. Yue, *An H^2 convergence of a second-order convex-splitting, finite difference scheme for the three-dimensional Cahn-Hilliard equation*, Commun. Math. Sci., 14: 489–515, 2016.

[27] D. He, K. Pan, and X. Yue, *A positivity preserving and free energy dissipative difference scheme for the Poisson-Nernst-Planck system*, J. Sci. Comput., 81:436–458, 2019.

[28] T. Horng, T. Lin, C. Liu, and R. Eisenberg, *PNP equations with steric effects: A model of ion flow through channels*, J. Phys. Chem. B, 116:11422–11441, 2012.

[29] J. Hu and X. Huang, *A fully discrete positivity-preserving and energy-dissipative finite difference scheme for Poisson-Nernst-Planck equations*, Numer. Math., 145:77–115, 2020.

[30] Y. Hyon, B. Eisenberg, and C. Liu, *A mathematical model for the hard sphere repulsion in ionic solutions*, Commun. Math. Sci., 9:459–475, 2010.

[31] X. Ji and S. Zhou, *Variational approach to concentration dependent dielectrics with the Bruggeman model: Theory and numerics*, Commun. Math. Sci., 17:1949–1974, 2019.

[32] M. Kilic, M. Bazant, and A. Ajdari, *Steric effects in the dynamics of electrolytes at large applied*

voltages. II. Modified Poisson-Nernst-Planck equations, Phys. Rev. E, 75:021503, 2007.

[33] B. Li, *Continuum electrostatics for ionic solutions with nonuniform ionic sizes*, Nonlinearity, 22: 811–833, 2009.

[34] B. Li, P. Liu, Z. Xu, and S. Zhou, *Ionic size effects: Generalized Boltzmann distributions, counterion stratification, and modified debye length*, Nonlinearity, 26:2899, 2013.

[35] X. Li, Z. Qiao, and C. Wang, *Convergence analysis for a stabilized linear semi-implicit numerical scheme for the nonlocal Cahn-Hilliard equation*, Math. Comp., 90:171–188, 2021.

[36] T. Lin and B. Eisenberg, *A new approach to the Lennard-Jones potential and a new model: PNP-steric equations*, Commun. Math. Sci., 12:149–173, 2014.

[37] C. Liu, C. Wang, S. Wise, X. Yue, and S. Zhou, *A positivity-preserving, energy stable and convergent numerical scheme for the Poisson-Nernst-Planck system*, Math. Comp., 90:2071–2106, 2021.

[38] H. Liu and Z. Wang, *A free energy satisfying finite difference method for Poisson-Nernst-Planck equations*, J. Comput. Phys., 268:363–376, 2014.

[39] B. Lu and Y. Zhou, *Poisson-Nernst-Planck equations for simulating biomolecular diffusion-reaction processes II: Size effects on ionic distributions and diffusion-reaction rates*, Biophys. J., 100:2475–2485, 2011.

[40] P. Markowich, *The Stationary Semiconductor Device Equations*, Springer-Verlag, 1986.

[41] M. Metti, J. Xu, and C. Liu, *Energetically stable discretizations for charge transport and electrokinetic models*, J. Comput. Phys., 306:1–18, 2016.

[42] A. Prohl and M. Schmuck, *Convergent discretizations for the Nernst-Planck-Poisson system*, Numer. Math., 111:591–630, 2009.

[43] Y. Qian, C. Wang, and S. Zhou, *A positive and energy stable numerical scheme for the Poisson-Nernst-Planck-Cahn-Hilliard equations with steric interactions*, J. Comput. Phys., 426:109908, 2021.

[44] Y. Qiao, B. Tu, and B. Lu, *Ionic size effects to molecular solvation energy and to ion current across a channel resulted from the nonuniform size-modified PNP equations*, J. Chem. Phys., 140:174102, 2014.

[45] R. Samelson, R. Temam, C. Wang, and S. Wang, *Surface pressure Poisson equation formulation of the primitive equations: Numerical schemes*, SIAM J. Numer. Anal., 41:1163–1194, 2003.

[46] R. Samelson, R. Temam, C. Wang, and S. Wang, *A fourth order numerical method for the planetary geostrophic equations with inviscid geostrophic balance*, Numer. Math., 107:669–705, 2007.

[47] J. Shen and J. Xu, *Unconditionally bound preserving and energy dissipative schemes for a class of Keller-Segel equations*, SIAM J. Numer. Anal., 58:1674–1695, 2020.

[48] J. Shen and J. Xu, *Unconditionally positivity preserving and energy dissipative schemes for Poisson-Nernst-Planck equations*, Numer. Math., 148:671–697, 2021.

[49] F. Siddiqua, Z. Wang, and S. Zhou, *A modified Poisson-Nernst-Planck model with excluded volume effect: Theory and numerical implementation*, Commun. Math. Sci., 16:251–271, 2018.

[50] Y. Sun, P. Sun, B. Zheng, and G. Lin, *Error analysis of finite element method for Poisson-Nernst-Planck equations*, J. Comput. Appl. Math., 301:28–43, 2016.

[51] R. Temam, *Navier-Stokes Equations: Theory and Numerical Analysis*, AMS, 2001.

[52] C. Wang and J.-G. Liu, *Convergence of gauge method for incompressible flow*, Math. Comp., 69: 1385–1407, 2000.

[53] C. Wang and J.-G. Liu, *Analysis of finite difference schemes for unsteady Navier-Stokes equations in vorticity formulation*, Numer. Math., 91:543–576, 2002.

[54] C. Wang, J.-G. Liu, and H. Johnston, *Analysis of a fourth order finite difference method for incompressible Boussinesq equations*, Numer. Math., 97:555–594, 2004.

[55] C. Wang and S. Wise, *An energy stable and convergent finite-difference scheme for the modified*

phase field crystal equation, SIAM J. Numer. Anal., 49:945–969, 2011.

[56] L. Wang, W. Chen, and C. Wang, *An energy-conserving second order numerical scheme for nonlinear hyperbolic equation with an exponential nonlinear term*, J. Comput. Appl. Math., 280:347–366, 2015.

[57] S. Wise, *Unconditionally stable finite difference, nonlinear multigrid simulation of the Cahn-Hilliard-Hele-Shaw system of equations*, J. Sci. Comput., 44:38–68, 2010.

[58] S. Wise, C. Wang, and J. Lowengrub, *An energy stable and convergent finite-difference scheme for the phase field crystal equation*, SIAM J. Numer. Anal., 47:2269–2288, 2009.

[59] J. Zhang, C. Wang, S. Wise, and Z. Zhang, *Structure-preserving, energy stable numerical schemes for a liquid thin film coarsening model*, SIAM J. Sci. Comput., 43:A1248–A1272, 2021.

[60] J. Zheng and M. Trudeau, *Handbook of Ion Channels*, CRC Press, 2015.

[61] S. Zhou, Z. Wang, and B. Li, *Mean-field description of ionic size effects with non-uniform ionic sizes: A numerical approach*, Phys. Rev. E, 84:021901, 2011.